British Journal of Healthcare and Medical Research - Vol. 11, No. 2
Publication Date: April 25, 2024
DOI:10.14738/bjhmr.112.16760.
Mayevsky, A. (2024). The Involvement of Carbon Monoxide in Mitochondrial Activity and Brain Functions. British Journal of Healthcare and Medical Research, Vol - 11(2). 121-154.

SERVICES FOR SCIENCE AND EDUCATION

The Involvement of Carbon Monoxide in Mitochondrial Activity and Brain Functions

Avraham Mayevsky
The Mina & Everard Goodman Faculty of Life Sciences and the Leslie and Susan Gonda Multidisciplinary Brain Research Center, Bar-Ilan University, Ramat-Gan 5290002, Israel

ABSTRACT

The central nervous system is the most sensitive tissue to carbon monoxide and usually receive the greatest lasting damage from CO poisoning. In the current set of experiments, the differences between the physiological responses and the toxic effects were studied. The effects of 1000, 2000 and 3000 ppm CO were studied in rats monitored by a unique multiparametric monitoring system providing information on the hemodynamic, metabolic, ionic and electrical activities in an un-anesthetized state. The effect of cortical spreading depression following the exposure to CO was investigated. The results show that exposure to 1000 ppm CO for 40 minutes doesn't have a deleterious effect on the resting brain but apparently interfere with metabolic activity during brain activation by cortical spreading depression. Exposure to 2000 ppm CO resulted in elevation of cerebral blood flow. The stability of mitochondrial NADH redox level during CO exposure indicated that tissue hypoxia did not develop. The elevation in blood flow was inhibited by L-nitroarginine methyl ester, indicating that nitric oxide was responsible for the CO-induced elevation in blood flow. Exposure to 2000 ppm CO also triggered a significant decrease in pH and rise in extracellular potassium ion, possibly due to ion-pump inhibition. The amplitude of the electrocorticogram wave activity decreased, indicative of a compromise to physiological activity.

Keywords: Brain energy metabolism, mitochondrial redox state, cerebral blood flow, aging rats, brain ion homeostasis, cortical spreading depression, brain electrical activity

INTRODUCTION

During the last few years, several lines of evidence have led to the suggestion that carbon monoxide (CO) may act as a neural messenger in a manner very similar to nitric oxide (NO) [1-4]. The physiological vs. toxic effects of CO apparently depend on the pharmacodynamics of this molecule in the various tissues. The central nervous system is the most sensitive tissue to CO and usually receives the greatest lasting damage from CO poisoning [5]. Carbon monoxide (CO) has been shown to effectively compete with O2, for hemoglobin binding. However, the propensity for CO to cause a hypoxic stress does not explain all of its clinical effects, as no correlation has been found between mortality and morbidity and the carboxyhemoglobin (COHb) level [4, 6-9].

The physiological versus toxic effects of CO apparently depend on the pharmacodynamics of this molecule. At least some adverse effects from CO exposure are due to an elevation of steady

state levels of NO, which appears to be due to competition between CO and NO for target sites rather than arising due to a direct stimulation of NO synthesis [10-15]. The clinical effects of toxic exposure to CO are dependent on the age of the patient [16]. In this study we, therefore, have investigated the toxic effects of CO on the central nervous system using our animal [17, 18]. Our hypothesis is that blood flow levels as well as its regulation vary in the aging rat. In order to test CBF regulation, the responses to low levels of CO were tested. We have limited this initial study to the effect of 2000 ppm CO, because it shows the most complex effect including an increase in CBF as well as inhibition of the Na-K-ATPase via possible uncoupling of the mitochondria. To accomplish this, we performed a study in which aging rats were exposed to 2000 ppm CO while monitoring brain functions using the multiparametric monitoring system [18].

Since brain energy stores are very limited [19] and the brain is absolutely dependent upon oxygen supply via cerebral blood flow (CBF), exposure to high concentrations of CO results in an increase in the CBF [20, 21], which may be partially due to lack of oxygen. Studies using relatively low concentrations of CO have demonstrated that the autoregulatory increase in blood flow [22] is sufficient for maintaining adequate cerebral oxygen supply [23]. Most of the studies on the effects of exposure to CO on brain energy metabolism have been carried out using relatively high concentrations of CO (2% or more). These studies report depletion of brain energy stores [24, 25], intracellular acidosis [26] as well as significant increases in the NADH/NAD+ ratio [27] and impairment of mitochondrial activity [28, 29]. Little information is available on brain energy metabolism under low CO concentrations in general and on the effect of CO on the activated brain in particular. Inducing cortical spreading depression (SD) is one way of causing brain activation and increasing oxygen demand [30]. SD is a phenomenon that has been described in the literature as a depression of spontaneous electrical activity [31]. It is accompanied by increased metabolic activity [32-36], changes in cerebral blood flow [37-39] and fluctuations in ionic homeostasis [40-42]. We have recently reported the recording of SD in a patient suffering from severe head injury [43].

The Aim of the Paper

The current paper is summarizing results accumulated in 5 different studies performed in our laboratory. The aim of the paper is to summarize the relationship between Carbon Monoxide-CO and brain CBF, Mitochondrial function and ionic homeostasis as well as electrical activities.

METHODS

The experimental protocols included in the current studies are presented in Table 1. As can be seen in the table, in three studies the multiparametric monitoring assembly was used. In the other 2 studies 2-channel and four channels fluorometer/reflectometer were used.

Table 1: Experimental and technical details of the studies protocols

Reference to the Technology	Monitoring System	Monitored Organ	Monitored Parameters	Treatments
337	MPA	Brain	CBF, NADH, Extracellular K^+, Ca^{2+}, H^+ ECoG	1000 ppm CO 3000 ppm CO Spontaneous CSD

4003	MPA	Brain	CBF, NADH, Reflectance, Extracellular K^+, H^+, ECoG	2000 ppm CO
4008	MPA	Aging Brain	CBF, NADH, Reflectance, Extracellular K^+, Ca^{2+}, H^+	2000 ppm CO
336	MPA 2 Channel Fluorometry	Brain	CBF, NADH, Extracellular K^+, Ca^{2+}, H^+, ECoG	3000 ppm CO Hyperbaric oxygenation
552, 343	MSMP	Brain	4 channel NADH Reflectance, DC potential	1000 ppm CO CSD

MSMP–Multi Site Multiparametric; CSD–Cortical Spreading Depression; MPA–Multiprobe Assembly; DC – Direct Current Steady Potential

Multiprobe Assembly (MPA)

To monitor all the required parameters from the same cortical tissue, we used a multiprobe assembly that was developed in our laboratory. Hemodynamic responses were monitored with laser Doppler flowmetry (LDF), which allows real-time and continuous monitoring [44-46]. The metabolic state of the brain was evaluated by monitoring the intramitochondrial redox state by using NADH surface fluorometry reflectrometry [27, 47-49]. Ionic homeostasis was measured by real-time monitoring of extracellular levels of K+, Ca2+ and Na+, or H+. The electrical status of the cortex was measured by electrocortiography (ECoG) and direct current (DC) steady potential. It is very hard to calculate the volume of tissue sampled by each of the probes used. Nevertheless, we found a very significant correlation between changes in the various parameters monitored under defined conditions such as ischemia, hypoxia, or spreading depression (SD) [50-54]. Therefore, we believe that the sampling volumes of the various probes are very similar to each other. The electrode holder for the MPA was a modified Lucite cannula that was originally described by Crowe et al. [55] for a light guide and a potassium-sensitive electrode. To allow space for more probes, the new cannula was shaped as a truncated cone instead of a cylinder (Fig. 1A). The holes accommodating the short electrode probes (K+, Ca2+, Na+, or H+) converged toward the lower surface of the holder to occupy less space on the brain. A divergent orientation at the top of the cannula facilitated handling and sealing of the probes [52, 53]. An additional hole was drilled obliquely from the upper surface to merge with each sensor channel at about mid distance from the lower surface. This hole accommodated the polyethylene tubing used to record the local DC potential concentric to the sensor. The long and rigid steel stem of the light guide used in this study occupied a straight vertical hole in the cannula and served as an axis to hold the cannula and the cable holder at a convenient distance from each other. Threaded steel rods were used as additional pillars to fix the cannula to the cable holder. The arrangement left optimal access to the electrodes and electrical connections for assembling and replacement. The complete assembly was protected and shielded by an aluminum sleeve that was placed over the cable holder. Once the electrodes were in place, the DC channel and the lower part of the sensor channel were filled with electrolyte solution from a lateral hole connected to a reservoir. Thus, we could ensure that each sensor and DC electrode was tightly sealed to the top of the cannula to prevent electrolyte reflow back into the cable housing compartment. The system also allowed the extracellular fluid and blood to be cleaned from the slit around each probe after the cannula was removed from an implantation site. In

URL: http://dx.doi.org/10.14738/bjhmr.112.16760.

the final assembly (Fig. 1A), a protective sleeve was used as an anchoring point for the refill tubes to the DC and sensor channels and for the reference liquid junction.

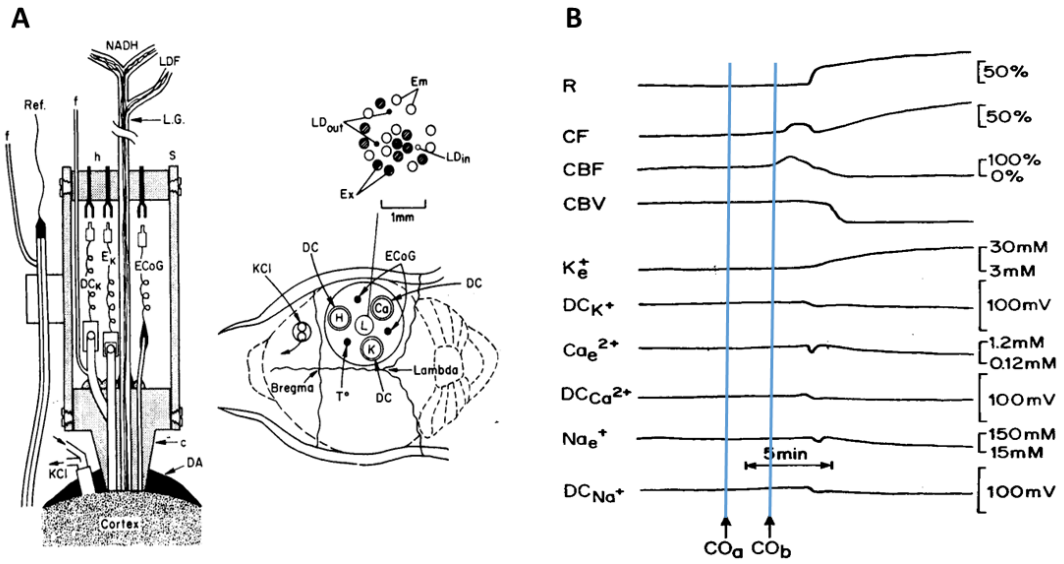


Figure 1A: Multiprobe assembly used in awake rat to monitor hemodynamic, metabolic, ionic, and electrical activities from the brain. Left: longitudinal section. Right: location of multiprobe assembly on the skull. Ref - reference electrode; f - feeling tube of reference or other direct current electrodes; h - connectors holder; NADH - 2 arms of NADH monitoring light guide; LDF - laser Doppler flowmeter; L - light guide; s - aluminum sleeve; DCK and EK - direct current and ion specific electrodes, respectively, for K; ECoG - electrocortical electrodes; c - Plexiglas probe holder; DA - dental acrylic cement; KCl - push-pull cannula for KCl; K, Ca, and H - ion specific electrodes; DC - area of direct current steady potential monitoring; Ex and Em - excitation and emission fibers, respectively, for NADH monitoring; LD_{in} and LD_{out} -optical fibers for monitoring blood flow and volume, respectively; To - termistor for local temperature measurement [92]. 1B: Exposure of an awake rat to a high dose of CO (>90%). Initial dose of CO was given at COa and was not so effective as second dose (COb) that was lethal [17].

Local Cerebral Blood Flow (CBF)

To measure in real time, the CBF from the same cortical area as the MPA location, we used the LDF technique [44-46]. The LDF measures relative flow changes, and readings have been shown to correlate with the relative changes in CBF measured by the two other quantitative approaches (for a review see Ref. [46]). The principle of the LDF is to utilize the Doppler shift, namely, the frequency changes that light undergoes when reflected by moving red blood cells. A beam of low-power or diode laser light is transmitted by an optical fiber to the tissue. After the multiple scattering of the light, another optical fiber picks up the reflected light that is recorded by a photodetector. The run signal is analyzed by a complicated algorithm developed by the manufacturers, and the results are presented in percentage of a full scale (0-100%), thereby providing arbitrary relative flow values. The change in the total back-scattered light is an indirect measure of the blood volume in the sampled tissue. To quantitate and normalize CBF values, we defined the reading value after death as 0 CBF. The 100% value was defined as percent CBF read on the LDF scale during the control period before exposure to the treatment.

NADH Redox State Fluorometry

The principle of NADH monitoring from the surface of the brain is that excitation light (366 nm) is passed from the fluorometer to the brain via a bundle of optical fibers made of quartz. The emitted light (450 nm), together with the reflected light at the excitation wavelength, is transferred to the fluorometer via another bundle of fibers. The changes in the reflected light (R) are correlated to the changes in tissue blood volume and also serve to correct for hemodynamic artifacts appearing in the NADH measurement. An increase in R is due to less absorption of light by the tissue because of decrease in blood volume and vice versa. The changes fluorescence and reflectance signals are calculated relative to the calibrated signals under normoxic conditions. This type of calibration is not absolute but provides reliable and reproducible results from different animals and between different laboratories. More details on this technique have been published by our group [27, 48, 49, 56]. The combination of NADH and LDF techniques has been in routine use in our laboratory.

Ion-Selective Electrodes

To monitor the extracellular levels of K^+, Ca^{2+}, Na^+ and H^+, we used specially designed mini electrodes made by World Precision Instruments (WPI; Sarasota, FL). A flexible tubing made of polyvinyl chloride was sealed at one end with a membrane sensitive to a specific ion. The tube was filled with the appropriate solution and connected to an electrode holder with a salt bridge between the membrane and an Ag-AgCl pellet located inside the holder. The interface between the polyvinyl chloride tubing and the holder was glued with epoxy, and such electrodes were usable for a few weeks. The sensitivity of the electrodes to the specific ion was close to the Nernstian value, namely, 50-60 mV/decade for K^+, Na^+, Ca^{2+} and H^+ or 25-30 mV/decade for Ca^{2+}.

DC Steady Potential Electrode

DC potential was measured concentrically around the ion selective electrodes (K^+, Ca^{2+}, Na^+, H^+). Each electrode had a saline bath around its perimeter, and an Ag-AgCl electrode (WPI) was connected to it.

ECoG

Spontaneous electrical activity of the brain surface was measured by two polished stainless-steel rods or silver wire inserted into the MPA. Figure 13B shows typical response of the brain to exposing the rat to carbon monoxide environment [17].

Monitoring of NADH and DC Potential in Four Locations

Multisite Assembly

The aim of this study was to investigate the changes in the metabolic, hemodynamic and the electrical activities of cortical spreading depression- CSD wave propagation through the entire ipsilateral cortex in real time, and the effects of ethanol administration on these processes [57]. To this end, we constructed and applied a multisite assembly (MSA) to investigate the mechanism of propagation of the CSD phenomenon continuously and simultaneously, from four parasagittally arranged adjacent areas through the entire rat hemisphere, during a series of CSD cycles. This approach enabled us to determine whether the brain's metabolic, hemodynamic and electrical responses to CSD stimulation, spread homogeneously from its source to the other cortical areas and helped us determine the rate of CSD wave propagation before and after ethanol administration in the awake rat.

URL: http://dx.doi.org/10.14738/bjhmr.112.16760.

The MSA shown in Figure 2A was constructed in order to monitor mitochondrial NADH redox state and DC steady potential from four subsequent areas in the same cerebral hemisphere [49, 58]. It contains four bundles of optical fibers (1.26 mm O.D. × 0.31 mm I.D.) connected to a four-channel fluorometer-reflectometer providing information on the mitochondrial NADH redox state (surface fluorometry) as well as on tissue absorption properties (reflected light) from the four parasagittal arranged adjacent points (Fig. 2B). DC steady potential was monitored from four points located parallel to the four light guides, via Ag/AgCl electrodes (1.27 mm O.D. X 0.86 mm I.D.) relative to an Ag/AgCl reference electrode [42, 59].

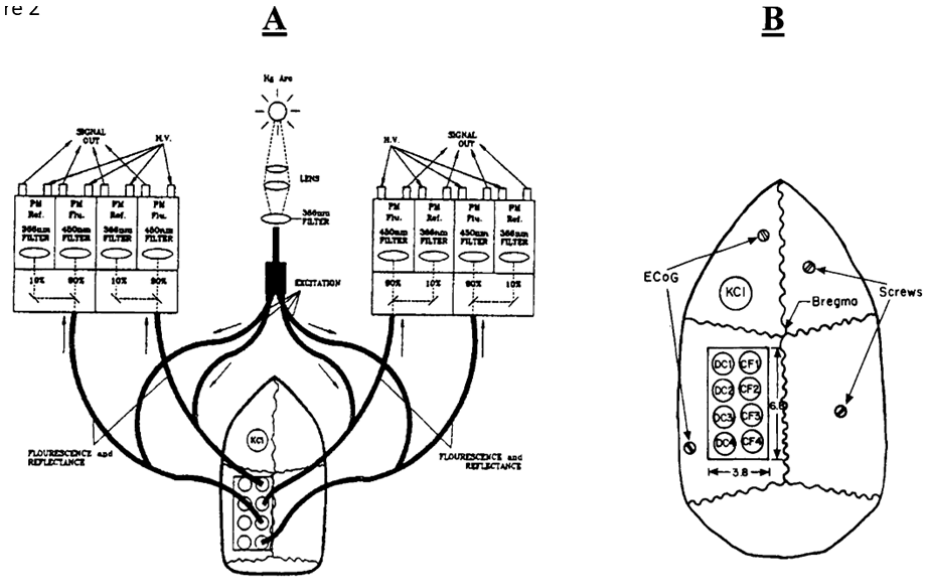


Figure 2: Schematic illustration of the multisite assembly system (MSA). (A) A four-channel DC fluorometer /reflectometer was connected to the rat brain using flexible fiber optic bundles for detecting mitochondrial NADH and light reflectance (changes from four parasagittal adjacently arranged areas). The system contains one mercury lamp (Hg Arc) light source and 366 nm filter for excitation, and 366 nm (for reflectance - Ref) and 450 nm [for fluorescence (Flu)] filters to measure emitted light, and photomultipliers (PM). HV. - High voltage. (B) The MSA system contains four light guides (CF1-CF4) and four DC electrodes (DC1-DC4). KCI - Push pull cannula; ECoG - for bipolar ECoG (electrocorticography) recording; screws - for MSA attachment to the skull [58].

NADH Redox State Fluorometry

For monitoring NADH redox state from the surface of the brain, 366 nm excitation light was passed from a fluorometer to the brain via a bundle of quartz optical fibers. The emitted light (450 nm), together with the reflected light at the excitation wavelength, was transferred to the fluorometer via another bundle of fibers. The changes in the reflected light are inversely correlated to changes in tissue blood volume and also serve to correct for hemodynamic artifacts appearing in the NADH measurement. Details on this technique have been described previously [27, 60, 61]. For measuring four areas simultaneously, the excitation light was divided to four bundles using a single light source (Fig. 2A).

Propagation of CSD waves on the cerebral cortex (of a control untreated animal) showed typical biphasic waves in the reflected light, an oxidation-reduction waves in NADH fluorescence, a negative shift in DC potential and a depression in ECoG (Fig. 17). It can be seen that the CSD

wave propagated from the first channel (closest to initiation area in the frontal lobe) towards the fourth, with a time delay of approximately 20–30 s between two adjacent channels [58].

CO Exposure Procedure

The rat was placed in an airtight Plexiglas cage. The CO at different concentrations in air (analyzed and certified by the manufacturer) was connected and flushed through the chamber. In preliminary experiments, the required level of CO was adjusted by mixing CO and air using flowmeters. In the present study, three groups of rats were used. The preliminary set of experiments was done at the University of Pennsylvania while the other two studies were carried out at Bar-Ilan University. In the initial studies, we used a MPA unit containing K^+, Ca^{2+}, and Na^+ electrodes; the Na^+ electrode was later replaced by the H^+ electrode. The results shown in the paper were selected from 15 rats. Five rats were exposed to 60 min of 1,000 ppm of CO, two rats to 20 min of 3,000 ppm of CO, and the other eight rats to 40 min of 1,000 ppm followed by 20 min of 3,000 ppm of CO [62].

RESULTS

Typical Responses of the Brain to 1000 and 3000 ppm Carbon Monoxide

Figure 3A shows the responses of an awake rat exposed for 60 min to 1,000 ppm of CO. The main change recorded under 1,000 ppm CO was the increase in relative CBF. The CF was unchanged, suggesting no change in NADH redox state. The R and cerebral blood volume (CBV) were also very stable. The ionic homeostasis and DC potential were unaffected, as measured by the various electrodes.

Exposure of the rat to the combination between 1,000 and 3,000 ppm of CO led to the result shown in Figure 3B. In this rat, the response to 40 min of 1,000 ppm of CO led to similar responses, shown in Figure 3A, except for the changes in the R that were very clear. The decrease in the R signal suggests an increase in light absorption [63], although the CBV in this rat did not respond to 1,000 ppm of CO.

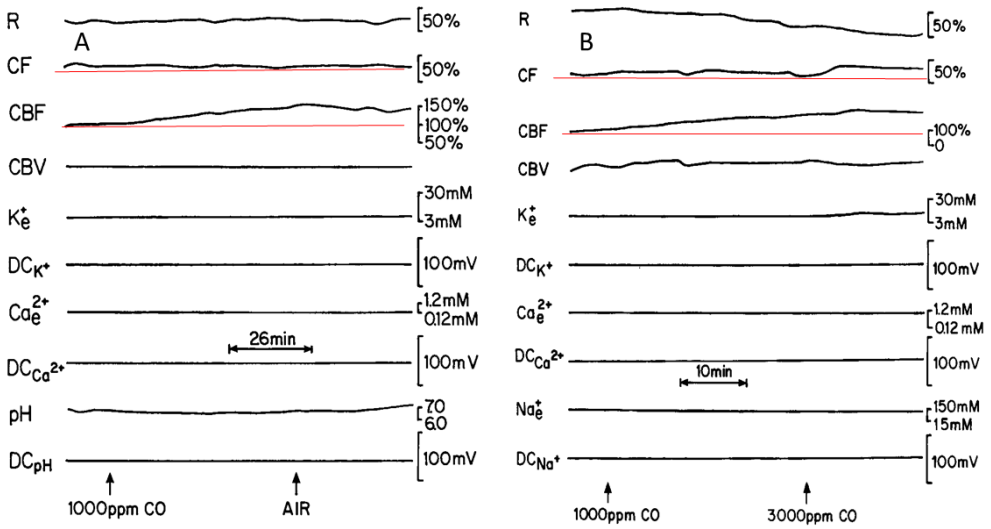


Figure 3: A - Responses to 60 min of 1,000 ppm of carbon monoxide (CO). R and CF, reflectance and corrected NADH fluorescence, respectively; CBF and CBV, cerebral blood flow and cerebral blood volume, respectively; K_e^+ and Ca_e^{2+}, extracellular levels of K^+ and Ca^{2+},

URL: http://dx.doi.org/10.14738/bjhmr.112.16760.

respectively; pH, extracellular level of H^+ ions expressed in standard units; DC_{K+}, $DCCa^{2+}$, and DC_{pH}, DC steady potential measured concentric to K^+, Ca^{2+}, and H^+ electrodes, respectively. CBV signal is presented without an ordinate due to nature of output of this signal. Laser Doppler flowmeter does not allow this signal to be calibrated. B - Effects of exposure to 1,000 ppm of CO followed by 3,000 ppm of CO on metabolic hemodynamic, ionic, and electrical activities measured in awake rat. R and CF, reflectance and corrected NADH fluorescence, respectively; CBF and CBV, cerebral blood flow and cerebral blood volume, respectively; K^+ and Ca^{2+} and Na^+ extracellular levels of K^+, Ca^{2+} and Na^+, respectively, expressed in standard units; DC_{k+}, $DC_{Ca2+,}$ and DC_{Na+} steady potential measured concentric to K^+, Ca^{2+}, and Na^+ electrodes, respectively. CBV signal is presented without an ordinate due to nature of output signal. Laser Doppler flowmeter does not allow this signal to be calibrated [17].

During the 1,000 ppm of CO period, the NADH was not affected at all, and only 3,000 ppm of CO led to an increase in NADH, suggesting a decrease in O_2 supply to the brain. Also, a small increase in K^+ was noticed under the 3,000 ppm of CO. The typical response of the spontaneous electrical activity to CO exposure is shown in the ECoG tracing in Figure 4. The main changes were recorded under 3,000 ppm of CO, although small changes did occur under 1,000 ppm of CO. During the 20-min period of 3,000 ppm of CO, the amplitude of the electrical activity was depressed to 50--60% of the original level. In this rat the ECoG did not show a depolarization event that occurred in many other rats (see below).

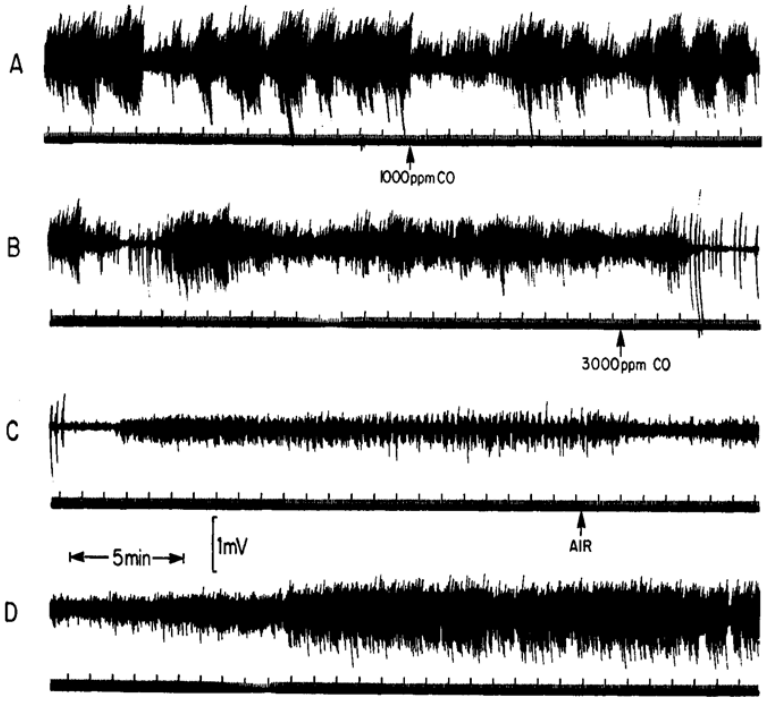


Figure 4: Responses of Electrocorticogram to 1,000 and 3,000 ppm of CO measured in awake rat. A-D, continuous recording of entire period [17].

Exposure of an awake rat to a high concentration of CO led to a lethal toxic effect, as shown in Figure 1B. The chamber was flushed twice with 90% CO levels. Before the death response, the CBF showed a large increase typical of the CO response, and immediately after the death response, the CBF went down to 0 level concomitantly with the NADH increase and ionic and electrical changes. A clear increase K^+ was followed by a decrease in Ca^{2+} and Na^+ as expected

under brain death. These changes in ion concentration are typical of a depolarization event that occurred under ischemia, anoxia, or severe asphyxia (see Ref. [64]). All three DC electrodes showed the typical negative shift that is also found in severe ischemia [50, 52, 54].

The majority of rats exposed for 40 min to 1,000 ppm of CO followed by 20 min to 3,000 ppm of CO demonstrated brain responses that were actually more severe than those shown in Figures 3A and 3B. Typically, 1,000 ppm of CO caused an increase in CBF while NADH, K^+, Ca^{2+}, and DC potential were stable (Fig. 5). Small acidification (pH) was also monitored during this period. Six to seven minutes after the exposure to 3,000 ppm of CO, a SD-like response or depolarization event was often recorded, and the extracellular level of potassium, K_e^+ showed a clear increase-decrease cycle together with negative wave in the DC potential. Under those conditions (3,000 ppm of CO), energy was still available to start recovery. In this animal, the Ca^{2+} electrode was not responding due to the very low sensitivity induced by an unclear reason. Also, the pH showed a very large decrease during the 3000 ppm of CO period. The brain had started to recover from the depolarization under CO, as seen by the decrease in K^+ and normalization of the DC potential. Under those conditions (3,000 ppm of CO), energy was still available to start recovery. In this animal, the Ca^{2+} electrode was not responding due to very low sensitivity induced by an unclear reason. Also, the pH showed a very large decrease during the 3,000 ppm of CO period. During the depolarization or SD event, the CBF trace showed a transient decrease. The NADH response was not clear, possibly due to the large increase in the R.

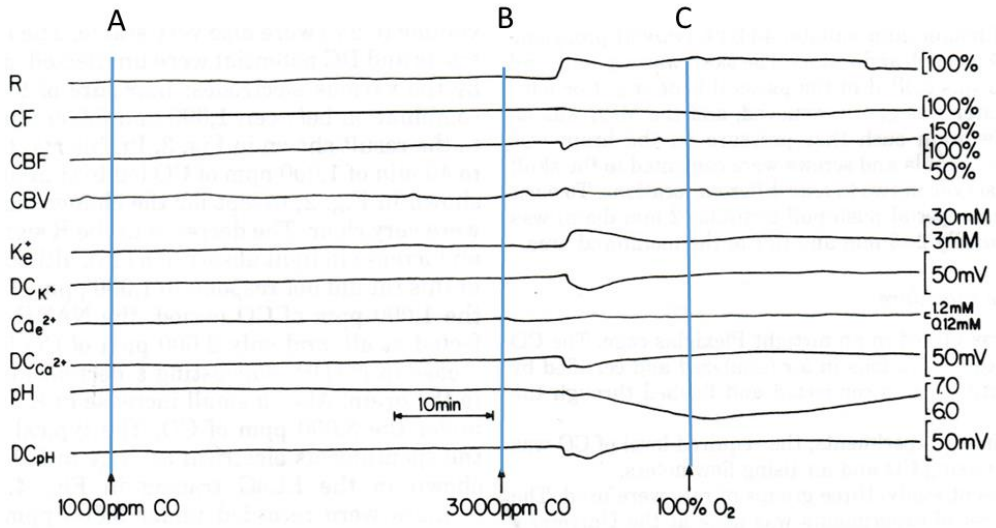


Figure 5: Responses to 40 min of 1,000 ppm of CO(A) followed by 20 min of 3,000 ppm of CO(B). To facilitate recovery, 100% O_2 was given (C) instead of air. In this experimental setup, Na+ electrode was replaced by H^+ electrode. In this experiment, Ca^{2+} electrode was not functioning properly for an unclear reason [17].

Effects of Anesthesia on Brain Responses to 2000 ppm CO-Statistical Analysis

A multiprobe assembly was used which allowed continuous monitoring of physiological variables during exposure to 2000 ppm CO. Typical responses, as presented in Figure 6A, include a prompt increase in CBF, slow leakage of potassium ions from the extracellular space, a slight oxidation of NADH (CF) and decrease in pH. A depolarization wave (D) was observed in 4 of the 7 animals in the final minutes of the planned 60 min exposure. Two spontaneous

URL: http://dx.doi.org/10.14738/bjhmr.112.16760.

spreading depression waves were observed in 3 of these 4 animals (a total of six waves). The depolarization was associated with continued leakage of potassium ions from the cells, a decrease in the DC potential, a large increase in the reflectance and a decrease in NADH fluorescence which has been shown to be an artifact of the reflectance changes, as well as a decrease in blood flow and pH [52, 65].

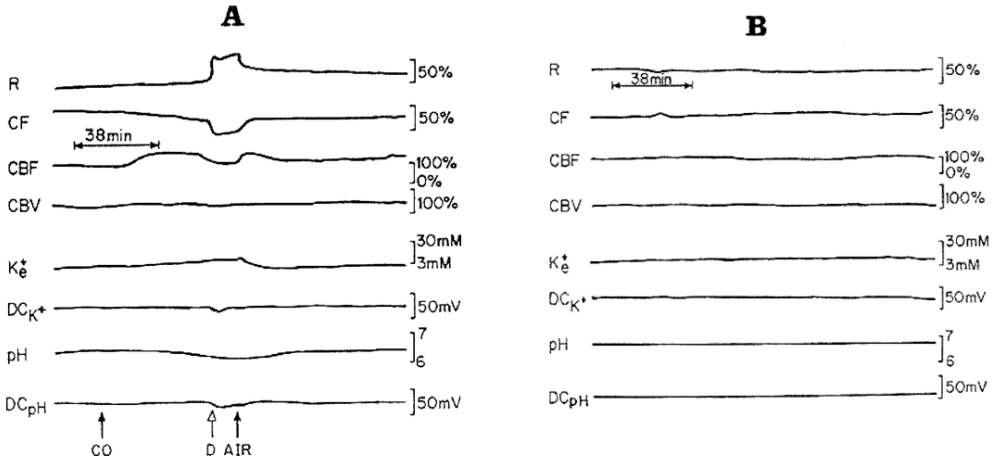


Figure 6: Tracing of the metabolic, hemodynamic and ionic responses of an awake animal. A: Exposure to 2000 ppm CO for 1h and recovery upon breathing air for another 2h. B: Control animal that breathed air for an equivalent period of time. R, reflectance at 366 nm; CF, corrected NADH fluorescence; CBF, CBV, relative blood flow and volume; DC, steady direct current potential measured concentric to the K^+ and H^+ electrodes; K^+, pH, extracellular ion concentration [106].

During the recovery phase, when rats breathed air after CO exposure, the NADH, CBF and potassium ion concentrations exhibited almost complete recovery. However, even among control rats, there was a gradual increase in extracellular potassium ion concentration and blood flow over the 3.5h study. The typical pattern of signals from a control rat (awake animal exposed to air only) is presented in Figure 6B. There were no statistically significant differences in values in control rats over the entire experimental period.

Quantitative Assessment of 2000 ppm CO Effects

Quantitative evaluations were carried out by determining the average changes in the six parameters monitored with the multiprobe assembly. They include reflectance (%), NADH (%), Cerebral Blood Flow (%), DK^+ (mM), DC_{K+} (mV) and DCpH. Mean values were calculated from recordings taken every 10 min for the entire experimental period. During exposure to CO there were significant increases in cerebral blood flow (CBF), DK^+, DCk^+, as well as decrease in DpH (Figs. 7A and 7B). There was small, no significant changes in the reflectance and NADH. A significant increase in CBF was maximal after 30 min of exposure (119±5.8 versus 179±13.7, $p<0.01$) and remained significantly high for 20 min. During recovery the reflectance returned to the pre-exposure levels and the marked elevation in CBF resolved.

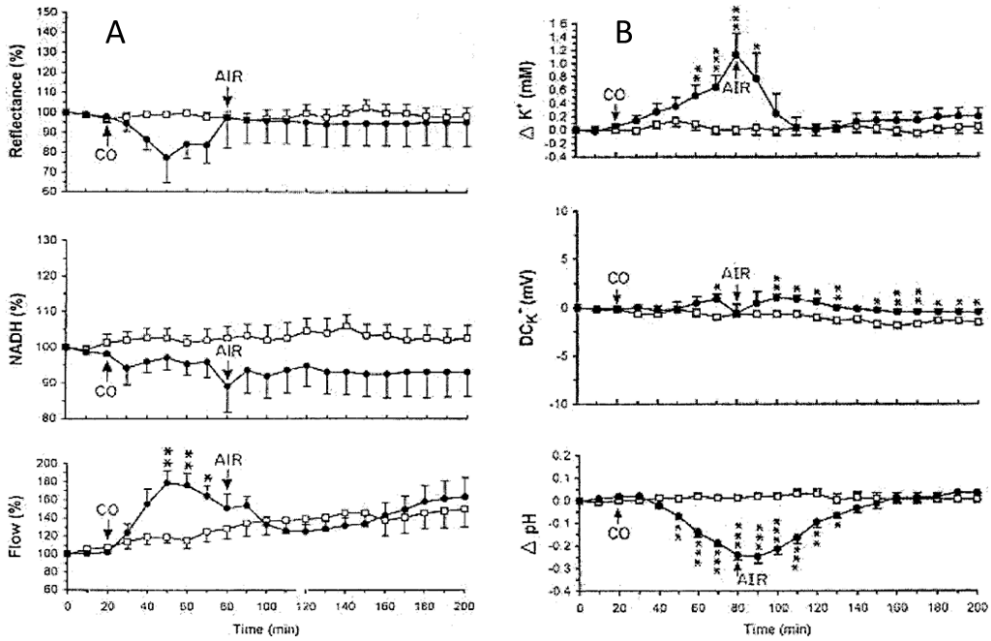


Figure 7: A: The reactions (in percentages) of the reflectance, NADH and cerebral blood flow in awake rats exposed to 2000 ppm CO (square) or air (circle). *p<0.05 between the experimental and the control group; **p < 0.01 between the experimental and the control group [106]. B: The reaction of the delta K^+, DC_K and delta pH in awake rats exposed to 2000 ppm CO (circle) or air (square). *p<0.05 between the experimental and the control group. **p<0.01 between the experimental and the control group. ***p<0.001 between the experimental and the control group [106].

Figure 7B demonstrates a significant increase in potassium ion concentrations after 40 min of exposure to 2000 ppm CO and complete recovery was observed only after breathing air. After 60 min of exposure to CO, potassium ion levels reached their maximal value. The pH demonstrated a significant decrease 30 min after exposure and complete recovery occurred only after breathing air for 50 min. DCK+ was increased after exposure for 50 min, whereas complete recovery was not observed even after breathing air at the end of the experiment.

CO and Anesthesia

There were no significant changes in the six monitored parameters when air-breathing rats were anesthetized with pentobarbital (nembutal) (Figs. 8A and 8B). When anesthetized rats were exposed to CO, no significant increases in the reflectance and NADH signal were observed which were similar to the changes seen in awake rats (Figs. 8A and 8B). A significant increase in blood flow was observed 30 min after exposure which was similar to the changes observed in awake animal exposed to CO. After 60 min, the increase was maximal (93±11.9 versus 178±19.5, p<0.01) and the maximum elevation in blood flow of the anesthetized animals (178% = 19.5%) was similar to that of the awake animals (179±13.7). It is notable that in the anesthetized animals, CO exposure did not cause significant changes from control in extracellular potassium, DC potential or pH (Fig. 8B).

URL: http://dx.doi.org/10.14738/bjhmr.112.16760.

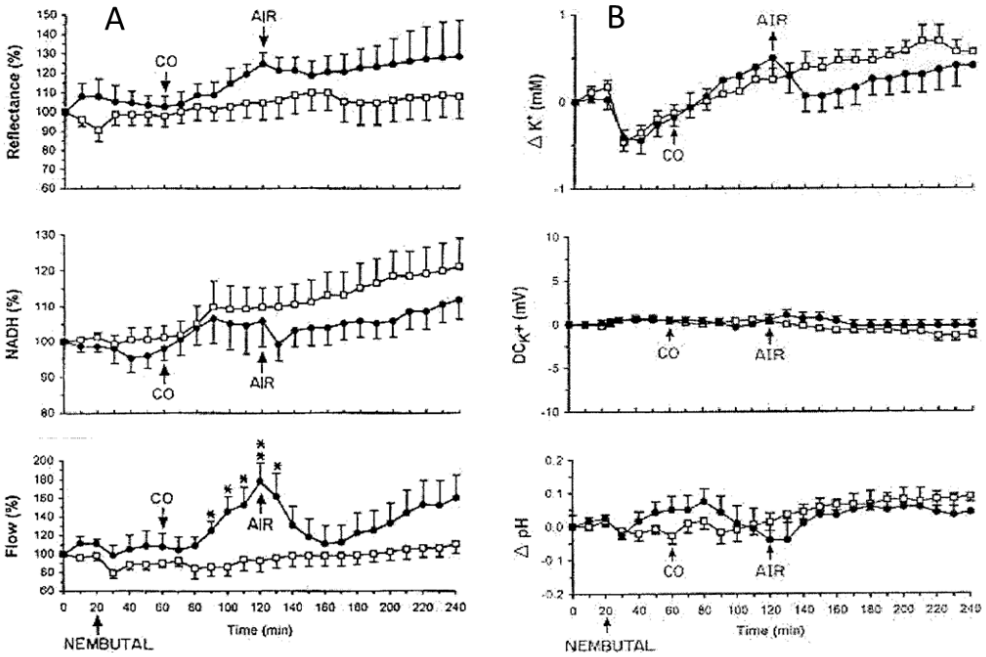


Figure 8: A: The reactions (in percentages) of the reflectance, NADH and cerebral blood flow in anesthetized rats exposed to 2000 ppm CO (circle) or air (square). *p<0.05 between the experimental and the control group; **p<0.01 the experimental and the control group [106]. B: The reaction of the Delta K^+, DC_{K+} and Delta pH in anesthetized rats exposed to 2000 ppm CO (circle) or air (square). No significant differences were observed [106].

Electrocorticogram

The electrocorticogram (ECoG) was monitored to provide a qualitative evaluation of brain electrical activity. The ECoG of an awake rat exposed to 2000 ppm CO for 1 hour is presented in Figure 9A.

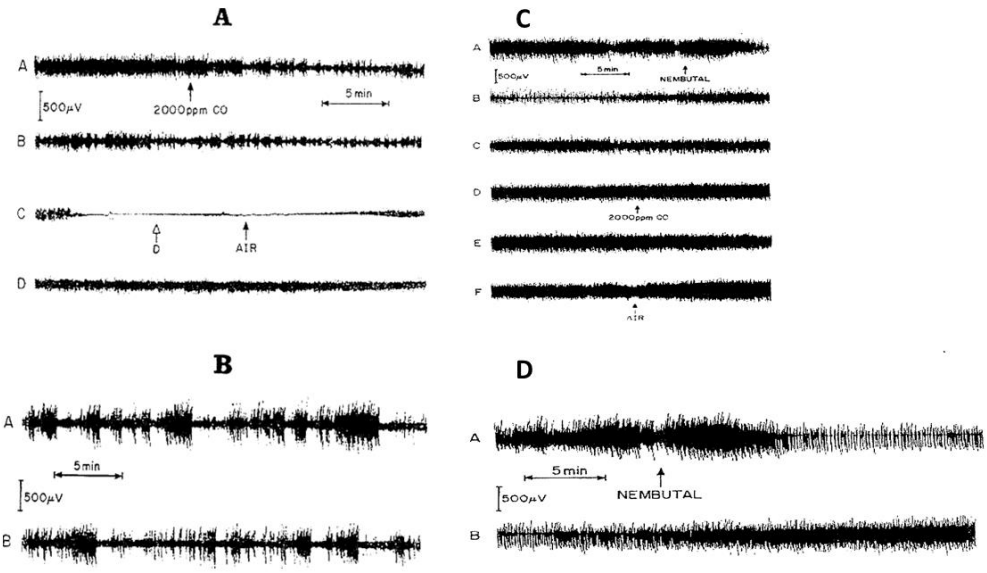


Figure 9: Tracing of continuous spontaneous electrical activity from the brain (ECoG). A: In an awake rat exposed to 2000 ppm (D, depolarization). B: In an awake rat exposed to air [106].

C: In an anesthetized rat exposed to 2000 ppm CO for 1h and recovery upon breathing air for another 2h. D: In an anesthetized rat exposed to air [106].

A progressive decline in the ECoG was observed during exposure to CO (C) and even more pronounced depressions in amplitude occurred during the episodic depolarization events (D). The ECoG of a typical control animal that was awake and exposed to air for the entire experiment is presented in Figure 9B. This tracing is for a shorter time period than that presented in Figure 9A, since no changes were observed in the ECoG during the entire experimental period.

Figure 9C presents the ECoG of an anesthetized animal injected with pentobarbital (Nembutal), a manipulation that caused reversible ECoG depression. Exposure to 2000 ppm CO after pentobarbital resulted in a different ECoG than in control animals that were not exposed to CO (Fig. 9D).

Responses of the Aging Brain to CO

The responses of adult rats (3 months of age) to 2000 ppm CO are presented in Figures 10 and 11.

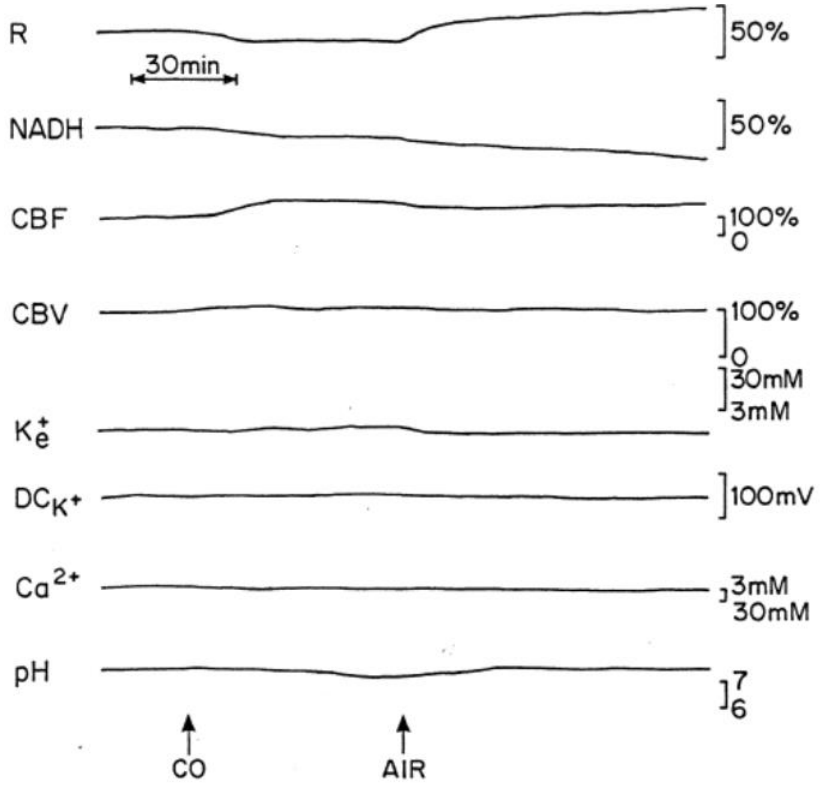


Figure 10: Tracing of the metabolic (NADH), hemodynamic (CBF)and ionic responses of an adult awake rat exposed 2000 ppm CO for 1 hour and recovery upon breathing air for another 2 hours. R - Reflectance at 366 nm, NADH - Corrected NADH fluorescence; CBF, CBV - Relative cerebral blood flow and volume; DC_{K+} - Steady direct current potential measured concentric to the K^+ electrode; K^+, Ca^{2+}, pH^+ - Extracellular ion concentration [18].

URL: http://dx.doi.org/10.14738/bjhmr.112.16760.

Figure 10 shows the responses, with respect to all of the parameters monitored for a single rat exposed to CO and Figure 11 shows the average results for both groups of adult animals. Figure 11 only shows the data for NADH, CBF, and potassium. These results show that the significant increase in CBF recorded previously under 1000 or 3000 ppm CO [17], is also observed under 2000 ppm. Thus, in Figure 10 a clear increase in CBF was recorded immediately after the exposure to CO with a partial recovery after re-breathing air. The decrease in the signal of the mitochondrial NADH indicates oxidation of NADH. There is a clear correlation between the increased CBF and the oxidation of NADH under CO environment. Although during the recovery phase, the CBF decreased, the NADH remained oxidized.

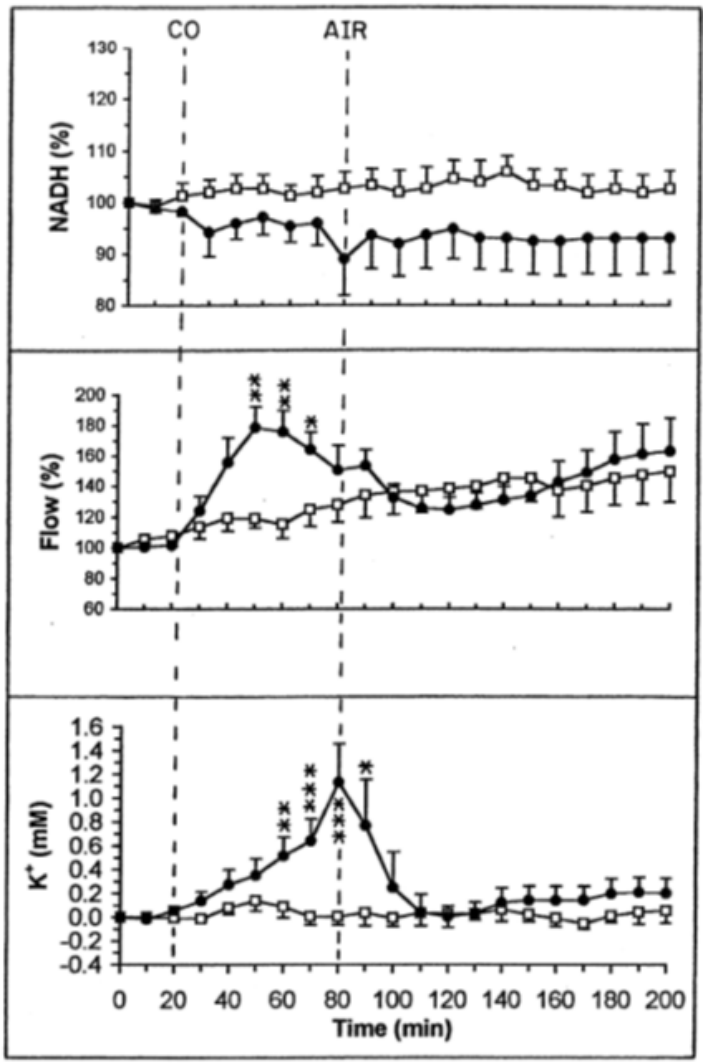


Figure 11: Responses of the adult rat brain to 2000 ppm (circle) or air (square). The main three parameters measured by the MPA, namely NADH, CBF and extracellular Delta K^+ (mM) are presented. Note that extracellular K^+ is expressed as Delta K^+ - values and in absolute values. *p<0.01, *p<0.05, ***p<0.001 between the experimental and the control group [18].

During the CO exposure period a small clear and reversible increase in extracellular K^+ was found together with a decrease in brain pH (Fig. 10). The detailed results and statistical analysis of the effects of 2000 ppm CO in the normal adult (3 months of age) rat are shown in Figure 11.

As can be seen, the NADH levels in the control group (air) were quite stable during the entire recording period (six rats). In the CO exposed group (seven rats) a small (not significant) decrease in the NADH levels without a recovery upon breathing normal air mixture was recorded. As can be seen in both groups a general trend (not significant) of increased CBF was recorded. Superimposed on this gradual increase, the CBF was elevated after CO breathing and the difference became significant at three-time intervals 30-50 min after the exposure to CO. The effect of 2000 ppm CO on extracellular K^+ was significant at four time points. Also, a significant decrease in pH was found between the CO exposed and control adult rats as seen in Figure 12. The detailed data will be published elsewhere together with more relevant data. After re-breathing air, the recovery of the ionic homeostasis to the baseline was observed.

The results for the aging rats (24 months of age) are presented in Figures 12A and 12B. In these figures a comparison is made between the responses of rats exposed to 2000 ppm CO (seven rats) as compared to control animals of the same age (five rats) allowed to breathe air for the entire experimental period.

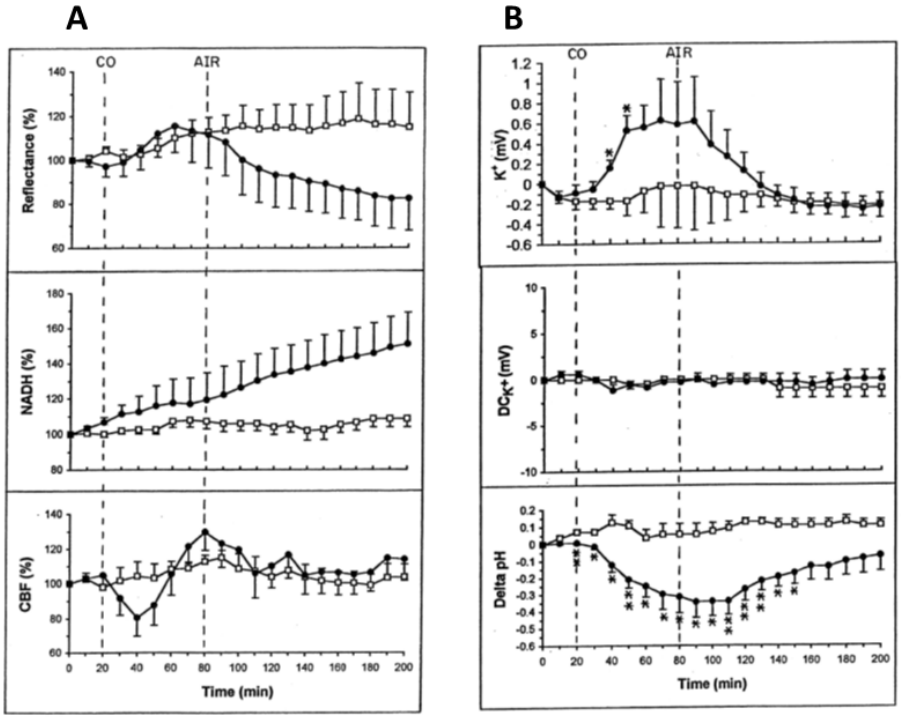


Figure 12: A: Graph presenting the responses (in percentages) of the reflectance, NADH and cerebral blood flow in aging rats exposed 2000 ppm (circle) or air (Square) [18]. B: Graph presenting the reaction of the delta K^+ (mM), DC_{K+} and pH in aging rats exposed 2000 ppm CO (circle) or air (square). Note that extracellular K^+ is expressed as delta K^+ values and not in absolute values. *p>0.05, **p>0.01 between the experimental and the control group [18].

In the aging rat, the CBF response was clearly different from that of the adult rat as shown in Figure 12A. During the 60 min exposure time to CO the CBF showed an insignificant decrease followed by an insignificant increase, meaning no significant difference in CBF was recorded during the entire period of exposure to CO.

URL: http://dx.doi.org/10.14738/bjhmr.112.16760.

The effects of 2000 ppm CO on the reflectance trace were insignificant as shown in Figure 12A. The NADH response to CO shown in Figure 12A is somewhat unique. Thus, even though the NADH signal increased during the entire course of the experiment for the CO group, during the 60 min of CO exposure, no significant change was recorded.

The effects of 2000 ppm CO on the extracellular K^+ levels for the aged rats (Fig. 12B) were similar to those found for the adult rats (Fig. 11). Thus, the exposure to CO led to a significant increase and complete recovery was recorded when air was returned.

The effects of 2000 ppm CO on the pH values in the old rats (Fig. 12B) show the same trend found for the adult rat (Fig. 12). Thus, the control air exposed old group was very stable during the monitoring period while the CO exposed group showed a significant decrease in pH and recovery when re-breathing air.

The results presented in Figure 12 were selected in order to emphasize the main difference between the adult and old age rats. The main significant difference was in the CBF response without any difference in the K^+ or H^+ responses, therefore only the K^+ presented in Figure 12.

CO Exposure and Cortical Spreading Depression (CSD)

In order to test the effect of brain activation on the various parameters, a wave of spreading depression was induced by epidural application of KCl solution [48]. The awake rat (at least 3 hours after the operation) was exposed to 1000 ppm CO in air for 40 minutes followed by 20 minutes of 3000 ppm CO [66]. The most significant effect of 1000 ppm CO was a large increase in CBF as measured by, the Laser Doppler flowmetry technique [67]. During this period, the NADH redox state, extracellular K^+ and Ca^{2+} as well as the DC steady potential were not affected. A slight acidification of brain surface was recorded. This increase in CBF was not recorded in control awake rats monitored during the same time period. A few minutes after changing to 3000 ppm CO a significant increase in NADH redox state was recorded and in the majority of studies 4 spontaneous spreading depression-like response occurred. We presume that the SD like response is due to disturbances in energy supply (increased CF signal) as depolarization wave developed. The same pattern of responses as recorded when the rat was exposed to 3000 ppm CO (without the 40 min of 1000 ppm CO exposure). In this case the NADH did show an Increase very soon after the exposure to CO although the CBF also increased at the same time. During the depolarization episodes, which were very similar to spreading depression, extracellular K^+ level increased concomitant with a shift in the DC steady potential. The metabolic and hemodynamic responses to this depolarization event were different from the typical response to SD [52, 55]. The response recorded during the control period, demonstrate the coupling between the maintenance of ionic homeostasis and the increase in CBF due to the activation of mitochondrial activity. The changes in extracellular K^+, Ca^{2+} and H^+ [64, 68] led to an increase in CBF and the oxidation of NADH (increase CF). The record shown in Figure 13B was measured in the same rat used for Figure 13A and illustrates depolarization episode which occurred after 23 minutes of 1000 ppm CO. In this animal CO intoxication led to 4 reversed change in NADH fluorescence during the depolarization event, namely, an increase-reduction of NADH [63] instead of a decrease (oxidation].

Similar observations were made in a number of other animals. The changes in the extracellular ions were much smaller than those occurring during control SD although the DC steady

potential changes during spontaneous events due to CO poisoning were similar as shown in A and B.

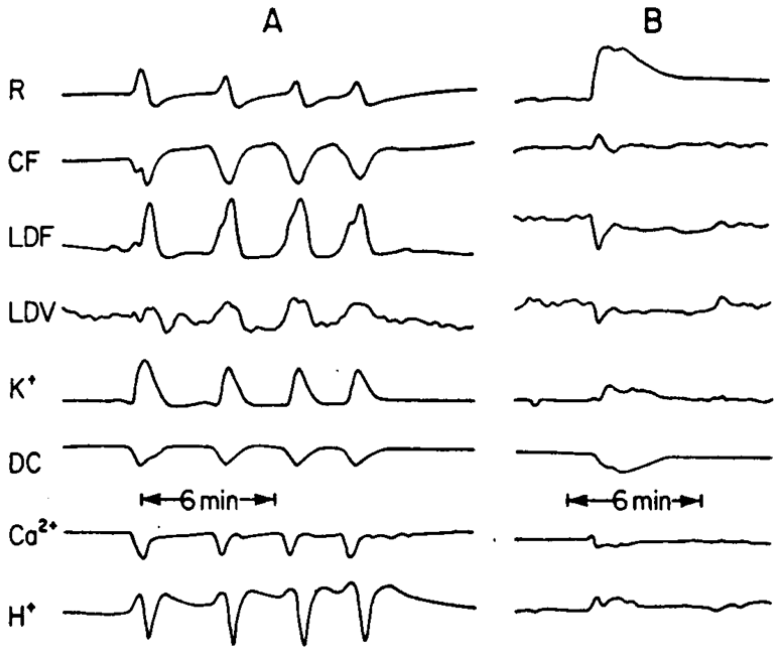


Figure 13: Two responses to spreading depression recorded during control (A) and 23 minutes after 1000 ppm CO Inhalation(B). R, CF: reflectance and corrected fluorescence. LDF, LDV: Cerebral blood flow and volume monitored by the Laser Doppler flowmeter. K^+, Ca^{2+}, H^+: extracellular levels of the three Ions. DC: Steady potential [107].

Another typical response to CO intoxication is shown in Figure 14A. In most animals exposed to 3000 ppm CO, oscillations in the hemodynamic and metabolic parameters were recorded. As seen, there is an inverse relation (180°) between the wave of CBF (LDF) and the NADH redox state (CF), suggesting that the blood supply is not stable and secondarily perturbates the intracellular redox state. The same pattern of oscillations has been recorded in rats exposed to bilateral carotid artery occlusion [69].

Another example showing the development of a SD like response is shown in Figure 14B. This rat was exposed directly to 3,000 ppm of CO and not to a preceding interval of 1,000 ppm of CO. The CBF was doubled and stayed at the high level during the entire exposure. Here again, the CBF showed a transient decrease during the depolarization event together with a short increase in NADH (CF). The lower NADH level after the wave suggests a degree of NADH oxidation. The fact that a clear decrease in the K^+_e trace was recorded suggests an activation of the Na^+-K^+-ATPase due to the SD or changes in K^+ permeability. Differences in the responses to spontaneously developed SD in air or different CO concentrations can be appreciated in Figure 15, where the patterns in one rat during different CO exposures are displayed. In Figure 15A, the rat was in an air-breathing environment and the changes in the ionic and metabolic responses were typical of SD. The responses shown in Figure 15B were recorded under 1,000 ppm of CO while those in Figure 15C were under 3,000 ppm of CO. The main changes among these conditions were in the hemodynamic responses, namely, that under CO the large hyperemic response to SD did not occur.

URL: http://dx.doi.org/10.14738/bjhmr.112.16760.

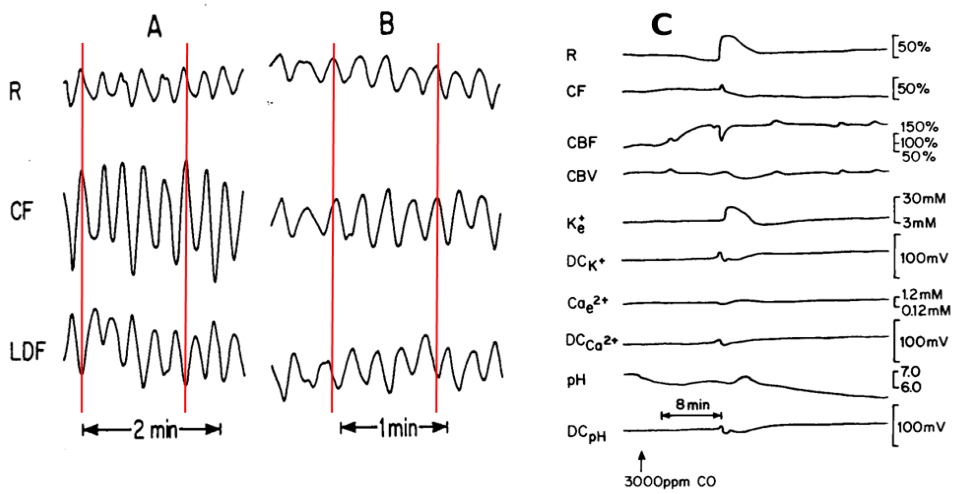


Figure 14: A, B: Metabolic and hemodynamic oscillations recorded after exposure to 3000 ppm CO. R, CF: reflectance and corrected fluorescence. LDF: Cerebral blood flow and monitored by the Laser Doppler flowmeter [107]. C: Exposure of an awake rat to 3,000 ppm of CO without pretreatment with 1,000 ppm of CO. Spontaneous spreading depression (SD)-like wave was developed under CO [17].

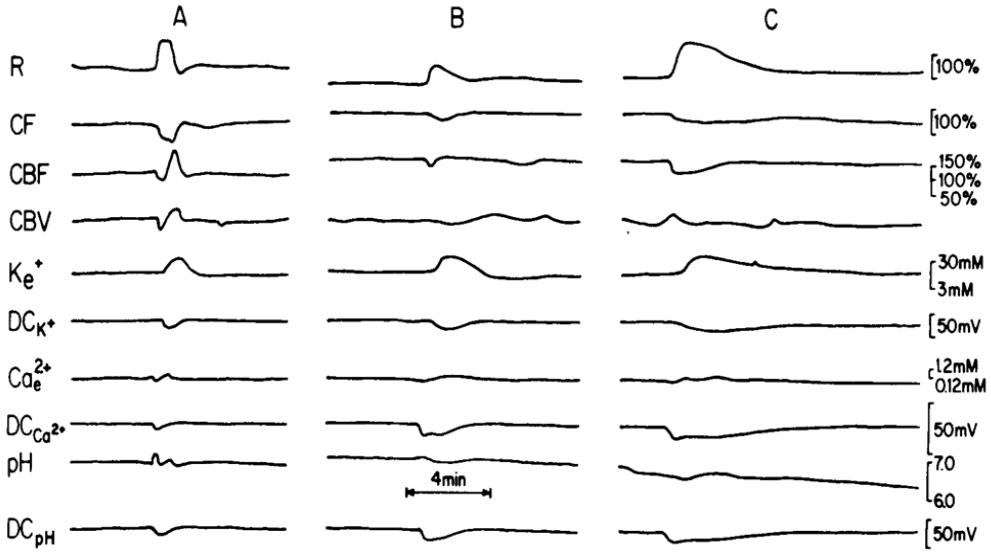


Figure 15: Responses to spontaneously developed cortical SD under air (A), 18 min of 1,000 ppm of CO (B), and 2.5 min of 3,000 ppm of CO (C). All scales in C are identical to A and B. Initiation of SD was spontaneous and was similar to other rats in which SD was induced by epidural washing of KCI solution 2-5 mm anterior to MPA [17].

Also, the duration of the wave was slower under CO, as seen by the various parameters. In another rat exposed to 1,000 ppm followed by 3,000 ppm of CO, spontaneous responses to SD waves were recorded. As seen in Figure 16, under 1,000 ppm of CO the responses to SD were very similar to normal control responses (Fig. 15A). In this animal, the Ca^{2+} did show clear responses to the SD. The appearance of the two SD waves under 1,000 ppm of CO did not affect the general trend of the clear increase in CBF. Under 3,000 ppm of CO, the CBF response was reversed, namely, that a large decrease was recorded instead of the large increase found under

1,000 ppm of CO. The R was also different under 3,000 ppm of CO, and the CFs were lower. The duration of the wave under 3000 ppm of CO was 3-4 times longer as measured by the DC potential trace. To show the quantitative effects of CO, we analyzed the results obtained from six rats exposed to the defined protocol. The rats were exposed to 1,000 ppm of CO for 40 min and then to 3,000 ppm of CO for 20 min. Parameters that demonstrated reproducible changes are shown in Table 2. CBF increased significantly in all rats under 1,000 ppm of CO ($p<0.05$) as well as under 3,000 ppm of CO ($p<0.005$). The NADH level was stable and unaffected by 1,000 ppm of CO, whereas 11±10.6% (SE) increase was recorded under 3,000 ppm of CO ($p<0.05$ by t-test). K^+_e was slightly elevated under 3,000 ppm of CO, but this change was significant ($p<0.05$ by t-test). The pH clearly changed under 3,000 ppm of CO but not with exposure to only 1,000 ppm of CO. Spontaneous SD waves were recorded in four of six rats while they were exposed to 1,000 ppm of CO. Spontaneous oscillations were recorded in five of the six rats of this group.

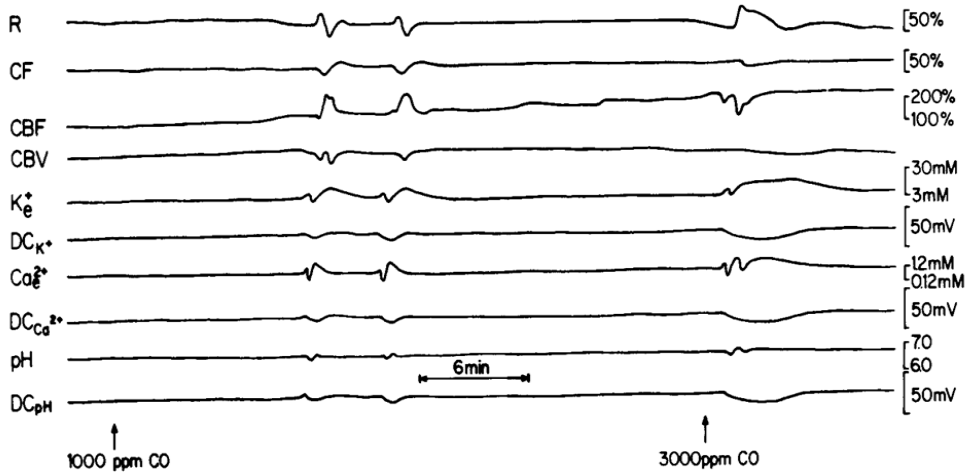


Figure 16: Spontaneous SD waves developed under 1,000 and 3,000 ppm of CO [17].

Table 2: Effects of 1000 ppm CO Followed by 3000 ppm on Various Parameters in 6 Awake Rats

	Rat Number						
	1	**2**	**3**	**4**	**5**	**6**	**Mean±SE**
	Flow, %						
Control	100	100	100	100	100	100	133±5.2
CO-1	132	123	127	150			
CO-2	150	123	148	150	172	120	144±7.2
	NADH, %						
Control	100	100	100	100	100	100	
CO-1	100	100	100	100			
CO-2	110	110	110	113	113	112	111±0.6
	K^+, mM						
Control	3.4	2.7	3.1		4.6		3.45±0.35
CO-1	3.4	2.5	3.2				
CO-2	3.6	4.6	6		5.4		4.90±0.45
	pH (acidic)						
CO-1	-	-	-	-			
CO-2	+	+	+	+	+	+	

URL: http://dx.doi.org/10.14738/bjhmr.112.16760.

	Spontaneous SD Oscillations						
CO-1	+	+	-	-	+	+	
CO-2	+	-	+	+	+	+	

CO-1, end of 1,000 ppm CO; CO-2, end of 3,000 ppm CO; SD, spreading depression. Plus (+), change in pH and recording of spontaneous SD oscillations; Minus (-), no change in pH and no recording of spontaneous SD oscillations [17].

Interaction Between CO and CSD: A Multisite Brain Monitoring

The aim of this study was to examine the effect of 1000 ppm CO on the metabolic and electrical activity of the rat brain *in vivo* and its interrelation with brain activity following induced SD waves. Rats were exposed to 1000 ppm CO and SD was induced at different times during and after exposure. In all animals, blood flow began increasing already after the first 10 min of exposure to CO. This increase was sustained until the end of exposure to CO and reached an average maximal level of 144% (n=21, 144±6%, $p<0.05$). Ten minutes after reventilating the cage with air, CBF remained elevated and was not significantly different from the maximal level (139±5%). Two hours after reventilating the cage with air, almost complete recovery was observed and blood flow neared its initial value (108±3%). Control rats that breathed air for the entire experimental period did not exhibit any change in blood flow, and at the end of this time period blood flow was very similar to control levels (n=8, 100±2%). The changes in blood flow in this study were not accompanied by changes in NADH levels. Figure 17 presents a tracing from a rat brain in which SD waves were induced before exposure to CO (Fig. 17A) and 90 min after cessation of exposure (Fig. 17B). It can be seen that when SD was induced 90 min after cessation of exposure to CO, the frequency of the SD waves increased.

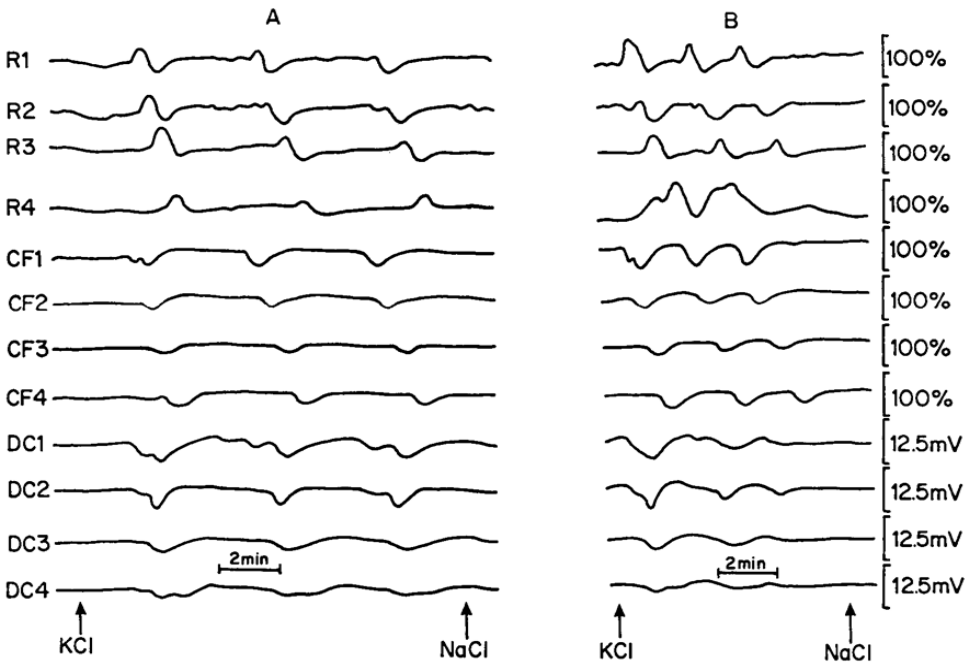


Figure 17: Tracing of the responses to cortical SD induced by flushing the brain with KCI in control animals (A), and 90 min after cessation of exposure to CO (B). RI, R2, R3, R4, reflectance; CF1, CF2, CF3, CF4, corrected NADH fluorescence; DC1, DC2, DC3, DC4, direct current potential measured in parallel to the NADH recorded from channels 1,2, 3, 4, respectively [22].

Rats in which SD was induced during exposure to CO did not exhibit any significant changes in the SD wave frequency as calculated from the NADH in all four channels (Fig. 18A). A significant decrease in the frequency of the NADH oxidation waves (CF waves) was observed in the rats of this group as compared to the waves induced before exposure to CO (mean of all four channels = 0.45±0.02 waves/min vs. 0.36±0.04; $p<0.02$) (Fig. 18B). These changes did not appear in the control rats; in which SD was induced at an equivalent time but were not exposed to CO. In contradistinction, rats in which SD was induced 90 min after cessation of exposure to CO exhibited a significant increase in the SD wave frequency (mean of all four channels = 0.35±0.02 waves /min vs. 0.47±0.02, $p>0.02$) (Fig. 18C). Similar changes were observed in the reflectance waves (R waves). The average changes in the R waves recorded during the SD episodes are presented in Table 2. The frequency of the DC waves in all experimental groups remained similar to that of the control groups. Group B, in which SD was induced immediately upon cessation of exposure to CO, was the only experimental group in which significant changes were observed in the amplitude of the NADH waves. A significant decrease was recorded in the amplitude of the CF (NADH) waves of the second SD wave (29±2.3 % average of four channels before exposure to CO vs. 18±2.4% after exposure, $p>0.05$) and of the third wave (28±0.9% before exposure to CO vs. 20.7±0.6% after exposure, $p<0.05$) (Table 3). The duration of the waves increased from 1.6 to 3 min (average of three first waves). Due to difficulties in calculating the integral of these NADH oxidation waves, it was calculated only for waves 2 and 3. This integral decreased significantly, apparently because of the decrease in wave amplitude, such that the total energy required was apparently decreased (Fig.19). The speed of propagation remained unchanged in all three groups.

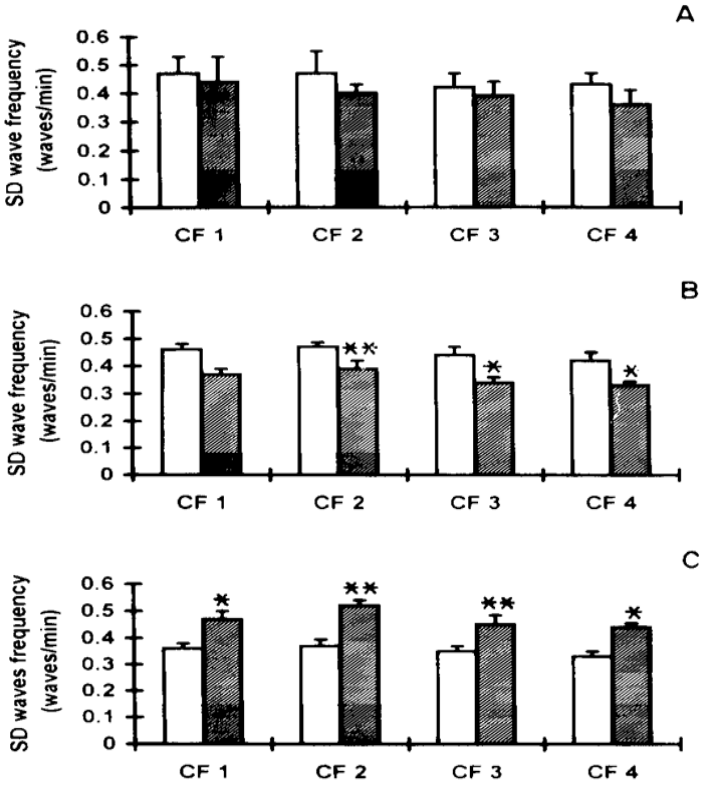


Figure 18: Histogram presenting the frequency of the SD waves (wave/min). CF1, CF2, CF3, CF4, corrected NADH fluorescence recorded from channels 1, 2, 3, 4, respectively. A: SD was induced during exposure of the animals to CO. B: SD was induced immediately upon cessation of

URL: http://dx.doi.org/10.14738/bjhmr.112.16760.

exposure to CO. C: SD was induced 90 min after cessation of the exposure. Light bars, control; dark bars, experimental animals. *p<0.05; **p<0.01 [22].

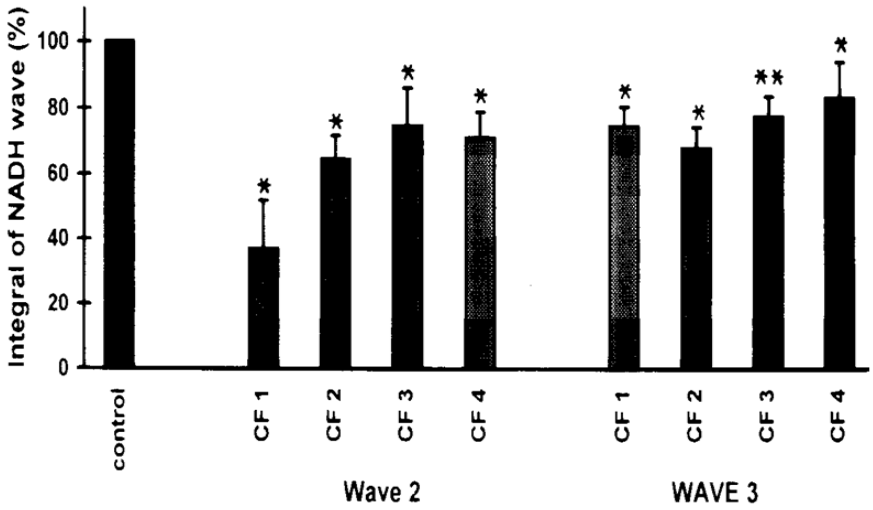


Figure 19: Histogram exhibiting the integral of the NADH waves before (control) and immediately after exposure to CO (waves 2 and 3). *p <0.05; **p <0.01 [22].

Table 3: Frequency of SD waves (waves/min) during (Group A), immediately after exposure to 1000 ppm CO (group B), and 90 min after cessation of exposure (group C)

		Group A	Group B	Group C
R1	Control	0.47±0.06	0.45±0.02	0.37±0.02
	After CO	0.44±0.09	0.36±0.02[b]	0.46±0.03[a]
R2	Control	0.47±0.08	0.44±0.02	0.35±0.02
	After CO	0.40±0.03	0.36±0.02[a]	0.48±0.03[b]
R3	Control	0.42±0.05	0.40±0.02	0.33±0.02
	After CO	0.39±0.05	0.33±0.01[b]	0.44±0.01[b]
R4	Control	0.43±0.04	0.40±0.02	0.33±0.01
	After CO	0.36±0.05	0.33±0.028	0.40±0.02[b]

R1, R2, R3, R4, reflectance of channels 1, 2, 3, 4, respectively. Data are represented as mean±S.E.M. [a] p<0.05; [b] p<0.01 [22].

Table 4: Changes in NADH amplitude during SD before (Control) and immediately after (CO) exposure to CO.

	Channels	Control	CO
WAVE 1	CF 1	17.42±2.1	15.5±4.25
	CF 2	15±3.5	11±0.25
	CF 3	23.75±6.6	21.24±4.9[a]
	CF 4	18.7±17	17±2.7
WAVE 2	CF 1	29.4±2.85	19.4±0.95[b]
	CF 2	31.4±7.6	19.3±0.75[b]

	CF 3	32.47±4.3	23.55±6.65[a]
	CF 4	28.6±8.8	20.6±4.85[a]
WAVE 3	CF 1	27.82±3.6	20.42±2.7[a]
	CF 2	27.9±7.95	18.8±3.95[b]
	CF 3	28.89±1.3	22.77±0.8[a]
	CF 4	27±6.05	21.05±9.05[b]

CF1, CF2, CF3, CF4, corrected NADH fluorescence recorded from channels 1, 2, 3, 4, respectively. All values are expressed as means ± S.E.M. of percent change. [a] $p<0.05$; [b] $p<0.01$ [22].

DISCUSSION

Brain Functions and Carbon Monoxide Exposure

The effects of CO on various brain biochemical and physiological activities were studied by various investigators by using independent protocols [70, 71]. Because the effects of CO are multifactorial, possibly including effects on mitochondrial activity [72], we adopted a multiparametric approach that allowed real time monitoring of various brain functions simultaneously. One of the known effects of CO in the 1000-3000 ppm range is a large increase in CBF. The mechanism for this is not clear. Ludbrook et al. [73] measured CBF and concluded that the primary toxicity of CO to the brain was not due to a reduction in O_2 delivery. MacMillan [74] concluded that the large increase in CBF under CO is due to tissue acidosis. Koehler et al. [23] suggested that hemoglobin-oxygen affinity plays a central role in determining blood flow. In all the published material, the level of CO in the mixture was on the borderline of hypoxic levels. In our present study, we exposed rats to a relatively low level of CO, 1,000 ppm or 0.1%, and compared the responses with those caused by 3,000 ppm of CO. The aim was to detect small changes in one or more of the many parameters monitored to assess the physiological role of CO, as suggested by Maines [1]. The standard exposure protocol, 1,000 ppm of CO for 40 min followed by 3,000 ppm of CO for 20 min, has been shown to cause oxidative stress [66]. In other studies, [66, 75], it was shown that exposure to 1,000 ppm of CO for 40-60 min will cause blood carboxyhemoglobin levels of 49±1% (n = 4). Exposure to 3,000 ppm CO for only 20 min is an inadequate time to significantly increase the blood level, and carboxyhemoglobin levels were found to be 54±3% (n = 7) [66, 75]. We have obtained data continuously and in real time during exposure to 1,000 ppm of CO alone or to 1,000 and 3,000 ppm of CO. The major response to 1,000 ppm of CO was an increase in CBF without any change in the oxidation reduction state of the mitochondria (NADH fluorescence). NADH fluorescence has been shown to be a very sensitive index of hypoxic stress in our ischemia models [50, 54, 67]. Normally, when the O_2 supply to brain cells is limited, the NADH should respond very fast, even when the inspired O_2 fraction was changed to 14-15% [76]. The NADH response is correlated very well to the CBF measured in the same tissue volume. It is well known that the Na^+-K^+-ATPase activity of the brain is responsible for at least 50% of total energy consumed [19], and we have shown that hypoxic stress will change the level of K^+_e [50, 54]. As shown in Table 2, K^+_e was stable under 1,000 ppm of CO. An absence of change in NADH or in K^+_e during exposure to 1,000 ppm of CO strongly suggests that changes in CBF were not due to hypoxia. We have found that exposure to 1,000 ppm of CO causes a 250-fold increase in the flux of NO from platelets [75]. Preliminary experiments currently being conducted in our laboratory suggest that the inhibition of NO synthase by an injection of nitroarginine before CO exposure blocks the CBF increase. We hypothesize that the responses in CBF (increase) at low concentrations of CO are not coupled to the energy deficiency as seen under hypoxia. Such a change in CBF may be regulated by a

URL: http://dx.doi.org/10.14738/bjhmr.112.16760.

mechanism similar to the one that causes NO to regulate CBF via a direct effect on smooth muscle [1, 77]. More studies are needed to clarify this point. For unclear reasons, the responses of the R and CBV were not so consistent among animals compared with those of the CBF and NADH. There was a slight increase in K^+_e under 3,000 ppm of CO, as well as an increase in NADH. Hence, under 3,000 ppm of CO, it appears that there may have been a marginal decrease in available energy. When the rat was exposed to 3,000 ppm of CO with or without the 40 min of 1,000 ppm, the change in CBF was dramatic and was accompanied by a small increase in NADH redox state (Fig. 14B). Spontaneous SD-like responses were often recorded, suggesting that a process of depolarization was initiated either by an insufficient energy supply or by the accumulated K^+ in the extracellular space. An alternative mechanism may involve the effects of increased intracellular Ca^{2+} that may occur due to an increased level of guanosine 3',5'-cyclic monophosphate induced by either the high CO level or the increased biosynthesis of NO [1].

Depolarization waves developed in all rats exposed to 3,000 ppm of CO and in four of six rats exposed to 1,000 ppm of CO (Table 3). The mechanism of the initiation of the SD or SD-like responses may be the same under 1,000 and 3,000 ppm of CO. However, as shown in Figures 15 and 16, the SD responses in the absence of CO, or with 1,000 ppm, were different from those found under 3,000 ppm of CO. The response to SD in the absence of CO and the usual response in the presence of 1,000 ppm of CO was a large transient hyperemia, whereas with 3,000 ppm of CO a short period of hypoperfusion occurred. This suggests that the ability of the brain to autoregulate CBF was impaired by CO when the microvasculature was nearly maximally vasodilated. In a few cases, the NADH response was also different, namely, an increase in NADH was recorded instead of a decrease (oxidation). We have found similar changes in the pattern of responses to SD in brains subjected to partial ischemia [41, 63]. Also, the appearance of the hemodynamic and metabolic oscillations demonstrated in Figure 14A were very similar to those found when ischemia was induced by carotid artery ligation in rats [69]. Significant correlations were found between four parameters showing the oscillations. The highest coefficient found was between CBF and CF ($r = -0.89$), whereas between CBF and R it was -0.85. These results suggest that the coupling between blood flow and NADH redox state (CF) was very high, as expected. The correlation coefficient between R, which represents mainly blood volume changes [27], and NADH (CF) was +0.58 and between R and CBV it was +0.38. All those coefficients were statistically significant ($p<0.01$). Under normoxic conditions we have never detected such an organized oscillation as in these four parameters. We are suggesting that CO exposure led to changes in the autoregulation of microcirculation and that the CBF was not stable. Those changes in CBF induced parallel changes in O_2 supply that were reflected in the oscillation found in the NADH levels.

Metabolic, Ionic and Electrical Responses to CO

The most prominent effects of exposure to 2000 ppm CO were an increase in blood flow and extracellular potassium ion concentration, and a decrease in pH. All these changes disappeared when animals were allowed to breathe air (Figs. 7A and 7B). The increase in blood flow was not accompanied by an elevation of basal NADH levels, which is an indirect measure of the oxidative state of the cells. Therefore, exposure to 2000 ppm CO is different from hypoxia even though hypoxia causes an increase in blood flow. During hypoxia a correlation has been found between oxyhemoglobin, tissue oxygen and NADH levels [27]. NADH levels also increase since the increase in blood flow is not sufficient to compensate for the oxygen deficiency, causing impairment of the respiratory chain. Several explanations can be proposed for the observed

stability in NADH during exposure to 2000 ppm CO. Oxygen extraction may be increased [30], or the increase in blood flow, mediated by NO based on the inhibitory potential of L-NAME, may be able to supply enough oxygen such that there is no change in oxygen consumption or oxygen supply to the tissue. Exposure to CO has been shown to elevate the steady state concentration of NO in both in vivo and in vitro experiments, and NO has a detrimental effect in that it contributes to oxidative stress from CO poisoning [78-83]. However, because 2000 ppm CO was only fatal to rats treated with L-NAME, NO has an important defensive role in CO poisoning. An increase in the extracellular potassium ion concentration was also observed during exposure to CO. This was not observed in L-NAME treated rats, indicating a role for NO in CO-induced potassium leakage. It is possible that potassium leakage was related to neuronal depolarization, as can be caused by membrane oxidative stress. Nitric oxide-derived oxidants have been shown to injure membrane integrity in *in vitro* studies and capillary integrity *in vivo* [80, 82, 83].

Alternatively, CO causes activation of the outward potassium channel in smooth muscle, and it may be that this also occurs in the CNS [84]. While a reduction in energy supply could cause ion leakage, this is less likely to have been affected by 2000 ppm CO because the respiratory chain was not impaired. However, it is also clear that CO causes adverse effects in the CNS that are independent of NO because L-NAME treated rats still exhibited a drop in brain pH. In the anesthetized animals exposed to 2000 ppm CO, the only change observed was an increase in the CBF, which disappeared during recovery breathing air. The peak in blood flow was similar to that observed in the awake animals upon exposure to CO. Extracellular potassium ion concentrations and pH did not change in the anesthetized animals. Possible explanations are that the anesthetic depresses either free radical formation and membrane oxidative stress, or CO-mediated activation of outward potassium channels as anesthetics may act as membrane stabilizers [85]. The ability to concurrently survey many brain parameters with the multiprobe assembly allows separation of alternative explanations for CO-mediated effects. Cerebral blood flow is increased by a NO-dependent mechanism which is not related to tissue hypoxia, based on the stability of brain NADH. Anesthesia inhibits leakage of potassium ions, the decrease in pH and the occurrence of spreading depression-like depolarization's during exposure to 2000 ppm CO. These CO-mediated effects were also unrelated to hypoxic stress, based on the absence of elevation in NADH redox state. We conclude that CO has at least three separable effects on cerebral function in rats. They include the classical hypoxic stress related to elevations in COHb and cardiac dysfunction that are found when levels of CO exceed 2000 ppm [23, 26, 74, 86, 87], effects related to elevations in steady state levels of NO and neuronal effects leading to reduction in pH that are inhibited by anesthesia.

CO Effects in the Aging Brain

The exact nature of the physiological and pathological effects of CO on the brain of adult animals or humans, at the cellular level, is still unclear. The influence of age on these physiological and pathological effects of CO have not previously been investigated even in animal models. Therefore, in the present study we investigated the effect of aging on the response to 2000 ppm CO, which has previously been investigated in adult rats [88].

It may be suggested that this increase in blood flow (in adult rats) is part of the regulatory response following oxygen deficiency [74, 86, 89]. However, this increase in blood flow is not accompanied by an elevation of basal NADH levels, which are an indirect measure of the oxidative state of the cells. Thus, the effect of exposure to 2000 ppm CO is distinct from the

URL: http://dx.doi.org/10.14738/bjhmr.112.16760.

effect of hypoxia. During hypoxia a correlation has been found between oxyhemoglobin, tissue oxygen, NADH levels [76]. Hypoxia resulted in increased blood flow, while NADH levels also increased [90]. This phenomenon is explained in terms of increased blood flow, which is not sufficient to compensate for the oxygen deficiency, causing impairment of the respiratory chain.

Several theoretical explanations can be proposed to explain the different relationships between the changes in blood flow and NADH. The increase in blood flow may be able to supply enough oxygen (no hypoxia) such that there is no change in the oxygen consumption or its supply to the tissue, and thus no change in NADH is observed. Furthermore, the increase in blood flow may be due to a dilatory agent (such as NO) which causes vasodilation independently of oxygen levels [62]. Another explanation may be that oxygen extraction is increased and this can maintain adequate tissue oxygen levels [30]. In fact, improved oxygen delivery can result in a decreased demand on the respiratory chain resulting in a decrease in NADH.

Koehler et al. suggest that an increase in the affinity of hemoglobin for oxygen, which takes place when CO binds to hemoglobin, impairs the delivery of oxygen and, thereby, plays a major role in blood flow regulation [23, 91]. The findings in this study do not support this theory since the increase in blood flow was not accompanied by changes in NADH in the adult rats.

In the present study we found that in the aging rats no significant change was observed in either CBF or NADH. These results indicate that aging influences the response to CO of CBF. We have already suggested that low levels of CO (1000 or 2000 ppm) affect the CBF in the adult rats via a non-hypoxic mechanism but rather through a NO dependent on NO involving process [92]. One of the possible explanations for the lack of clear CBF response to 2000 ppm CO in the aging rat is a weaker NO vasodilatory response in the old brain than in the adult brain. This conclusion is consistent with other reports in the literature. Toyoda et al. [93] showed, using laser Doppler flowmetry, that aging diminished the compensatory dilatation of brain stem arterioles during hypotension. The changes in CBF autoregulation in aging rats were studied also in spontaneously hypertensive animals. Fujishima et al. [94] found a diminished vasodilatory response of the brain to hypotension in 20-month-old rats.

The extracellular ionic environment was responsive to CO in both the aging rat and the adult rat (Figs. 11 and 12B). These findings demonstrate the strength of the multiparametric monitoring approach developed by us and applied to various pathological and physiological conditions [17, 43, 76, 95, 96]. The differentiation between the responses of the aging brain to CO seen in the energy metabolism and ionic homeostasis are very challenging. The fact that both extracellular K^+ and H^+ levels were elevated without a clear corresponding change in energy metabolism indicates that two different mechanisms or effects of CO may exist. The presence of more than one CO related process has previously [88] been suggested for the adult rat.

The increase in extracellular potassium ion concentration during exposure to CO without a change in NADH (Fig. 12A) indicates that the respiratory chain was not impaired and, therefore, ATP formation was not affected. Why then did the extracellular potassium ion concentration increase? Several explanations for this can be offered. As a result of the exposure to CO, free radicals are formed, changing the membrane permeability to ions [87] and a general depolarization of the cells occurs. This depolarization is expressed in a massive efflux of

potassium ions out of the cells accompanied by a decrease in pH, suggesting increased glycolysis and accumulation of lactic acid. Another possible explanation is that exposure to 2000 ppm CO directly activates an outward potassium channel, as shown for smooth muscle [97].

The effect of aging on brain energy metabolism has been studied. The vascular architecture of the brain shows a severe decrease in the vascularity of 124-week-old rats [98]. Using the gerbil brain exposed to complete ischemia, Buerk and Nair [99] found a significant decrease in O_2, consumption in the old animals (18-21 months). In another study, it was found that the infarct size in old rats)28-36 months) was larger as compared to the normal adult controls [100]. Ohata et al. [101] found that CBF was not significantly different between 24-month rats and 34-month rats. Parmacek et al. [102] found in 34-month mice a decrease in O_2, consumption as compared to normal adults (6 months). Sylvia and Rosenthal [103], using dual wavelength spectrophotometry, found that in rats, the resting mitochondrial redox state was not affected by age.

Responses to CSD After CO Exposure

One of the prominent effects of exposure of rats to a low concentration of CO is a transient increase in CBF [73]. In this study exposure to CO at a concentration of 1000 ppm for 40 min caused an increase in CBF but did not cause any measurable changes in the basal NADH redox levels, i.e., the normal metabolic activity of the brain was apparently not affected, since NADH is an inverse indicator of oxygen consumption and therefore energy metabolism. These results are in agreement with previous studies carried out in this laboratory [17, 92]. According to the literature, the carboxyhemoglobin level under these conditions is approximately 46% [5] and the increase in CBF may be part of an autoregulatory reaction to the decrease in oxygen supply. Mayevsky et al. [76] have shown that under other conditions in which the oxygen supply is restricted, such as during hypoxia, a correlation exists between oxyhemoglobin levels, tissue oxygen levels and NADH levels. The increased blood flow may have afforded sufficient compensation for the decrease in blood oxygen such that tissue hypoxia did not occur and therefore NADH levels remained stable. Increased oxygen extraction may also have increased the oxygen supply to the brain [30]. The fact that CBF began decreasing only a few minutes after the end of exposure to CO, although carboxyhemoglobin levels do not change so fast, suggests the participation of a dilatory agent (such as NO) with a direct effect on cerebral vessels [92, 104]. However, CO-hemoglobin levels or blood oxygen content were not measured in this study. In this study exposure to 1000 ppm CO for 40 min caused a decrease in the frequency of the induced SD waves as expressed by NADH waves, when the SD was induced immediately after cessation of exposure, whereas when SD was induced 1.5h after cessation of the exposure to CO the frequency of the waves increased. Exposure to CO may result in an impairment of the sodium–potassium pump which is expressed under conditions of increased ionic and metabolic activities, such as those existing during SD. The increased frequency of the waves observed 1.5h after reventilating the animals with air may be the result of the formation of free radicals which affect the ion permeability of the membrane [105]. In this study DC waves remained unchanged, negating the possibility that a decrease in the threshold potential of the tissue could increase SD wave frequency. This suggests that CO did not affect SD initiation. On the other hand, CO apparently interfered with recovery from SD (repolarization), which is an ATP-dependent state, as recorded from the changes in the frequency of the NADH waves and may explain the difficulty in recording three consecutive DC waves, since before complete recovery from one wave,

URL: http://dx.doi.org/10.14738/bjhmr.112.16760.

another wave may have already been initiated. The speed of propagation of both the NADH and the DC waves remained unchanged. This indicates that 1000 ppm CO did not affect the mechanism of propagation and that it did not result in an impairment of membrane permeability.

Activation of brain cells by inducing SD immediately after cessation of exposure to CO caused a smaller change in NADH oxidation than during the control SD waves. Although the duration of the waves increased, total energy expended decreased decrease in the CF wave integral. In contradistinction to hypoxia [27], in this study basal NADH levels remained stable and the integral of the CF waves decreased, indicating another possible source for ATP other than the respiratory chain, such as increased glycolysis. Another possibility for the increased energy supply is increased coupling between the respiratory chain and sodium potassium pump activity, i.e., a more efficient relation between energy formation and utilization. Furthermore, it must be pointed out that SD was induced after cessation of exposure to CO, at a time when no significant changes were recorded in the CBF, and the possibility that some of the above-mentioned changes may be due to reventilation cannot be ruled out. In order to clarify this point, studies are now being performed with the MPA system, which enables simultaneous measurement of ionic fluctuations during SD concomitantly to measuring CBF and NADH [76].

In conclusion, exposure to 1000 ppm CO for 40 min does not have a deleterious effect on the resting brain, but apparently interferes with metabolic activity during brain activation SD arousal. The results of this study indicate that 1000 ppm CO does not affect the SD initiation mechanism nor the SD propagation mechanism. However, it apparently has a delayed effect, which is expressed in a change in repolarization and energy metabolism during recovery from SD.

References

1. Maines, M.D., *Carbon Monoxide: An emerging regulator of cGMP in the brain.* Mol. Cell. Neurosci., 1993. 4(5): p. 389-97.

2. Baskaya, M.K., A. Dogan, and R.J. Dempsey, *Application of endovascular suture occlusion of middle cerebral artery in gerbils to obtain consistent infarction.* Neurol Res, 1999. 21(6): p. 574-8.

3. Manninen, H., et al., *How often does an incomplete circle of Willis predispose to cerebral ischemia during closure of carotid artery? Postmortem and clinical imaging studies.* Acta Neurochir (Wien), 2009. 151(9): p. 1099-105.

4. McCarty, R., *Letter: Magnesium deprivation and seizures in Mongolian gerbils.* J Gen Psychol, 1975. 92(1st Half): p. 3-4.

5. Penney, D.G., *Acute carbon monoxide poisoning: animal models: a review.* Toxicology, 1990. 62(2): p. 123-60.

6. Batchelder, M., et al., *The Laboratory Rabbit, Guinea Pig, Hamster, and Other Rodents; Gerbils.* National Library of Medicine., 2011.

7. Loskota, W.J., P. Lomax, and S.T. Rich, *The gerbil as a model for the study of the epilepsies. Seizure patterns and ontogenesis.* Epilepsia, 1974. 15(1): p. 109-19.

8. Sokal, J.A., et al., *Effect of different conditions of acute exposure to carbon monoxide on the cerebral high-energy phosphates and ultrastructure of brain mitochondria in rats.* Toxicol Lett, 1982. 11(3-4): p. 213-9.

9. Mathieu, D., et al., *Acute carbon monoxide poisoning. Risk of late sequelae and treatment by hyperbaric oxygen.* J Toxicol Clin Toxicol, 1985. 23(4-6): p. 315-24.

10. Ignarro, L.J., et al., *Nitric oxide as a signaling molecule in the vascular system: an overview.* J Cardiovasc Pharmacol, 1999. 34(6): p. 879-86.

11. Nagababu, E., et al., *Active nitric oxide produced in the red cell under hypoxic conditions by deoxyhemoglobin-mediated nitrite reduction.* J Biol Chem, 2003. 278(47): p. 46349-56.

12. Cosby, K., et al., *Nitrite reduction to nitric oxide by deoxyhemoglobin vasodilates the human circulation.* Nat Med, 2003. 9(12): p. 1498-505.

13. Nohl, H., et al., *Mitochondria recycle nitrite back to the bioregulator nitric monoxide.* Acta Biochim Pol, 2000. 47(4): p. 913-21.

14. Li, H., et al., *Characterization of the magnitude and kinetics of xanthine oxidase-catalyzed nitrite reduction. Evaluation of its role in nitric oxide generation in anoxic tissues.* J Biol Chem, 2001. 276(27): p. 24482-9.

15. Revelly, J.P., et al., *Endotoxic shock alters distribution of blood flow within the intestinal wall.* Crit Care Med, 1996. 24(8): p. 1345-51.

16. Posner, J.B., F. Plum, and A. Van Poznak, *Cerebral metabolism during electrically induced seizures in man.* Arch Neurol, 1969. 20(4): p. 388-95.

17. Mayevsky, A., et al., *Multiparametric monitoring of the awake brain exposed to carbon monoxide.* J. Appl. Physiol., 1995. 78: p. 1188-1196.

18. Mendelman, A., et al., *Brain multiparametric responses to carbon monoxide exposure in the aging rat.* Brain Res., 2000. 867(1-2): p. 217-222.

19. Erecinska, M. and I.A. Silver, *ATP and brain function.* J. Cereb. Blood Flow Metab., 1989. 9(1): p. 2-19.

20. Hawkins, M., J. Harrison, and P. Charters, *Severe carbon monoxide poisoning: outcome after hyperbaric oxygen therapy.* Br J Anaesth, 2000. 84(5): p. 584-6.

21. Kanten, W.E., et al., *Hemodynamic responses to acute carboxyhemoglobinemia in the rat.* Am J Physiol, 1983. 244(3): p. H320-7.

22. Meilin, S., et al., *Responses of rat brain to induced spreading depression following exposure to carbon monoxide.* Brain Res., 1998. 780(2): p. 323-328.

23. Koehler, R.C., M.D. Jones, Jr., and R.J. Traystman, *Cerebral circulatory response to carbon monoxide and hypoxic hypoxia in the lamb.* Am. J. Physiol., 1982. 243(1): p. H27-32.

24. Brown, S.D. and C.A. Piantadosi, *In vivo binding of carbon monoxide to cytochrome c oxidase in rat brain.* J,. Appl. Physiol., 1990. 68(2): p. 604-10.

25. Hardy, K.R. and S.R. Thom, *Pathophysiology and treatment of carbon monoxide poisoning.* J Toxicol Clin Toxicol, 1994. 32(6): p. 613-29.

26. Brown, S.D. and C.A. Piantadosi, *Recovery of energy metabolism in rat brain after carbon monoxide hypoxia.* J. Clin. Invest., 1992. 89(2): p. 666-72.

27. Mayevsky, A., *Brain NADH redox state monitored in vivo by fiber optic surface fluorometry.* Brain Res. Rev., 1984. 7: p. 49-68.

URL: http://dx.doi.org/10.14738/bjhmr.112.16760.

28. Piantadosi, C.A., P.A. Lee, and A.L. Sylvia, *Direct effects of CO on cerebral energy metabolism in bloodless rats.* J. Appl. Physiol., 1988. 65(2): p. 878-87.

29. Thom, S.R., et al., *Delayed neuropsychologic sequelae after carbon monoxide poisoning: prevention by treatment with hyperbaric oxygen.* Ann Emerg Med, 1995. 25(4): p. 474-80.

30. Mayevsky, A. and H.R. Weiss, *Cerebral blood flow and oxygen consumption in cortical spreading depression.* J. CBF Metab., 1991. 11: p. 829-836.

31. Leão, A.A.P., *Spreading depression of activity in cerebral cortex.* J. Neurophysiol., 1944. 7: p. 359-390.

32. Hansen, A.J., B. Quistorff, and A. Gjedde, *Relationship between local changes in cortical blood flow and extracellular K^+ during spreading depression.* Acta Physiol. Scand., 1980. 109(1): p. 1-6.

33. Mies, G. and W. Paschen, *Regional changes of blood flow, glucose, and ATP content determined on brain sections during a single passage of spreading depression in rat brain cortex.* Exp. Neurol., 1984. 84(2): p. 249-58.

34. Shinohara, M., et al., *Cerebral glucose utilization: local changes during and after recovery from spreading cortical depression.* Science, 1979. 203(4376): p. 188-90.

35. Rosenthal, M. and G. Somjen, *spreading depression, sustained potential shifts, and metabolic activity of cerebral cortex of cats.* J. Neurophysiol., 1973. 36: p. 739-749.

36. Mayevsky, A., D. Jamieson, and B. Chance, *Oxygen poisoning in the unanesthetized brain: correlation of the oxidation-reduction state of pyridine nucleotide with electrical activity.* Brain Res., 1974. 76: p. 481-491.

37. Dora, E., A. Koller, and A.G.B. Kovach, *Effect of topical adenosine deaminase treatment on the functional hyperemic and hypoxic responses of cerebrocortical microcirculation.* J. CBF Metab., 1984. 4: p. 447-457.

38. Shibata, M., C.W. Leffler, and D.W. Busija, *Cerebral hemodynamics during cortical spreading depression in rabbits.* Brain Res., 1990. 530(2): p. 267-74.

39. Wahl, M., M. Lauritzen, and L. Schilling, *Change of cerebrovascular reactivity after cortical spreading depression in cats and rats.* Brain Res., 1987. 411(1): p. 72-80.

40. Hansen, A.J. and T. Zeuthen, *Extracellular ion concentrations during spreading depression and ischemia in the rat brain cortex.* Acta Physiol. Scand., 1981. 113(4): p. 437-45.

41. Mayevsky, A., N. Zarchin, and C.M. Friedli, *Factors affecting the oxygen balance in the awake cerebral cortex exposed to spreading depression.* Brain Res., 1982. 236: p. 93-105.

42. Mayevsky, A., et al., *Brain mitochondrial redox state, tissue hemodynamic and extracellular ion responses to four-vessel occlusion and spreading depression in the rat.* Neurol. Res., 1990. 12: p. 243-248.

43. Mayevsky, A., et al., *Cortical spreading depression recorded from the human brain using a multiparametric monitoring system.* Brain Res., 1996. 740: p. 268-274.

44. Haberl, R.L., et al., *Laser-Doppler assessment of brain microcirculation: effect of systemic alterations.* Am J Physiol Heart Circ Physiol, 1989. 256: p. H1247-1254.

45. Dirnagl, U., et al., *Continuous measurement of cerebral cortical blood flow by laser-Doppler flowmetry in a rat stroke model.* J. CBF Metab., 1989. 9: p. 589-96.

46. Wadhwani, K.C., et al., *Blood flow in the central and peripheral nervous systems*, in *Laser Doppler Blood Flowmetry* A.P. Shephrd and P.A. Oberg, Editors. 1990, Kluwer Academic Pub: Boston. p. 265-304.

47. Chance, B. and G.R. Williams, *Respiratory enzymes in oxidative phosphorylation (I- Kinetics of oxygen utilization).* J. Biol. Chem., 1955. 217: p. 383-393.

48. Mayevsky, A. and B. Chance, *Metabolic responses of the awake cerebral cortex to anoxia hypoxia spreading depression and epileptiform activity.* Brain Res., 1975. 98: p. 149-165.

49. Mayevsky, A. and B. Chance, *Intracellular oxidation-reduction state measured in situ by a multicannel fiber-optic surface fluorometer.* Science, 1982. 217: p. 537-540.

50. Mayevsky, A., *Level of ischemia and brain functions in the Mongolian gerbil in vivo.* Brain Res., 1990. 524: p. 1-9.

51. Mayevsky, A., et al., *A fiber optic based multiprobes system for intraoperative monitoring of brain functions.* SPIE, 1991. 1431: p. 303-313.

52. Friedli, C.M., D.S. Sclarsky, and A. Mayevsky, *Multiprobe monitoring of ionic, metabolic, and electrical activities in the awake brain.* Am. J. Physiol., 1982. 243(3): p. R462-9.

53. Mayevsky, A., *Multiparameter monitoring of the awake brain under hyperbaric oxygenation.* J. Appl. Physiol, 1983. 54(3): p. 740-748.

54. Mayevsky, A., et al., *Brain vascular ionic and metabolic responses to ischemia in the Mongolian gerbil.* J. Basic Clin. Physiol. Pharmacol., 1990. 1: p. 207-220.

55. Crowe, W., A. Mayevsky, and L. Mela, *Application of a solid membrane ion selective electrode to in vivo measurements.* Am. J. Physiol., 1977. 233: p. C56-C60.

56. Mayevsky, A., *Brain energy metabolism of the conscious rat exposed to various physiological and pathological situations.* Brain Res., 1976. 113: p. 327-338.

57. Sonn, J. and A. Mayevsky, *The effect of ethanol on metabolic, hemodynamic and electrical responses to cortical spreading depression.* Brain Res., 2001/7/27. 908(2): p. 174-186.

58. Sonn, J. and A. Mayevsky, *The effect of ethanol on metabolic, hemodynamic and electrical responses to cortical spreading depression.* Brain Res., 2001. 908(2): p. 174-186.

59. Mayevsky, A., N. Zarchin, and J. Sonn, *Brain redox state and O_2 balance in experimental spreading depression and ischemia*, A. Lehmenkuhler, K.-H. Grotemeyer, and F. Tegtmeier, Editors. 1993, Urban & Schwarzenberg: Munchen-Wier, Baltimore. p. 379-393.

60. Mayevsky, A. and B. Chance, *Multisite measurements of NADH redox state from cerebral cortex of the awake animal.* Adv. Exp. Med. Biol., 1983. 159: p. 143-155.

61. Sonn, J., et al., *Effect of local ischemia on the myocardial oxygen balance and its response to heart rate elevation.* Quart. J. Exp. Physiol., 1982. 67: p. 335-348.

62. Thom, S.R. and L.W. Keim, *Carbon monoxide poisoning: a review epidemiology, pathophysiology, clinical findings, and treatment options including hyperbaric oxygen therapy.* J. Toxicol. Clin. Toxicol., 1989. 27(3): p. 141-56.

63. Mayevsky, A., *Ischemia in the brain: The effects of carotid artery ligation and decapitation on the energy state of the awake and anesthetized rat.* Brain Res., 1978. 140: p. 217-230.

64. Hansen, A.J., *Effect of anoxia on ion distribution in the brain.* Physiol Rev, 1985. 65: p. 101-148.

URL: http://dx.doi.org/10.14738/bjhmr.112.16760.

65. Chance, B., R.W. Estabrook, and A. Ghosh, *Damped sinusoidal oscillations of cytoplasmic reduced pyridine nucleotinde in yeast cells.* Proc. Nat. Acad. Sci., 1964. 51(6): p. 1244-1251.

66. Thom, S.R., *Carbon monoxide-mediated brain lipid peroxidation in the rat.* J. Appl. Physiol., 1990. 68(3): p. 997-1003.

67. Stern, M.D., et al., *Continuous measurement of tissue blood flow by laser-Doppler spectroscopy.* Am. J. Physiol., 1977. 232(4): p. H441-8.

68. Zarchin, N., et al., *Hemodynamic, metabolic, ionic, and electrical responses to cortical spreading depression in aging rats.* Adv. Exp. Med. Biol., 1999. 471: p. 223-230.

69. Mayevsky, A. and I. Ziv, *Oscillations of cortical oxidative metabolism and microcirculation in the ischaemic brain.* Neurol Res, 1991. 13(1): p. 39-47.

70. Bissonnette, B., et al., *Intracranial pressure and brain redox balance in rabbits.* Can. J. Anaesth., 1991. 38(5): p. 654-659.

71. Boyer, P.D. and H. Theorell, *The change in reduced diphosphopyridine nucleotide (DPNH) fluorescence upon combination with liver alcohol dehydrogenase (ADH).* Acta Chem. Scand., 1956. 10: p. 447-450.

72. Chance, B., M. Erecinska, and M. Wagner, *Mitochondrial responses to carbon monoxide toxicity.* Ann. N.Y. Acad. Sci., 1970. 174(1): p. 193-204.

73. Ludbrook, G.L., et al., *The relative effects of hypoxic hypoxia and carbon monoxide on brain function in rabbits.* Toxicology, 1992. 75(1): p. 71-80.

74. MacMillan, V., *Regional cerebral blood flow of the rat in acute carbon monoxide intoxication.* Can. J. Physiol. Pharmacol., 1975. 53(4): p. 644-50.

75. Thom, S.R., S.T. Ohnishi, and H. Ischiropoulos, *Nitric oxide released by platelets inhibits neutrophil B2 integrin function following acute carbon monoxide poisoning.* Toxicol. Appl. Pharmacol., 1994. 128(1): p. 105-10.

76. Mayevsky, A., et al., *Multiparametric evaluation of brain functions in the Mongolian gerbil in vivo.* J. Basic Clin. Physiol. Pharmacol., 1992. 3: p. 323-342.

77. Goadsby, P.J., H. Kaube, and K.L. Hoskin, *Nitric oxide synthesis couples cerebral blood flow and metabolism.* Brain Res., 1992. 595(1): p. 167-70.

78. Ischiropoulos, H., et al., *Nitric oxide production and perivascular nitration in brain after carbon monoxide poisoning in the rat.* J Clin Invest, 1996. 97(10): p. 2260-7.

79. Thom, S.R., S.T. Ohnishi, and H. Ischiropoulos, *Nitric oxide released by platelets inhibits neutrophil B2 integrin function following acute carbon monoxide poisoning.* Toxicol Appl Pharmacol, 1994. 128(1): p. 105-10.

80. Thom, S.R., et al., *Role of nitric oxide-derived oxidants in vascular injury from carbon monoxide in the rat.* Am J Physiol, 1999. 276(3): p. H984-92.

81. Thom, S.R., et al., *Adaptive responses and apoptosis in endothelial cells exposed to carbon monoxide.* Proc Natl Acad Sci U S A, 2000. 97(3): p. 1305-10.

82. Thom, S.R., et al., *Pulmonary vascular stress from carbon monoxide.* Toxicol Appl Pharmacol, 1999. 154(1): p. 12-9.

83. Thom, S.R., Y.A. Xu, and H. Ischiropoulos, *Vascular endothelial cells generate peroxynitrite in response to carbon monoxide exposure.* Chem Res Toxicol, 1997. 10(9): p. 1023-31.

84. Wang, R. and L. Wu, *The chemical modification of KCa channels by carbon monoxide in vascular smooth muscle cells.* J Biol Chem, 1997. 272(13): p. 8222-6.

85. Morgan, G.E. and M.S. Mikhail, *Neurophysiology and anesthesia*, in *Clinical Anesthesiology*, G.E. Morgan and M.S. Mikhail, Editors. 1992, Appleton and Lange: Norwalk, CT. p. 419–430.

86. MacMillan, V., *Cerebral energy metabolism during recovery from carbon monoxide hypoxia-oligemia.* Brain Res., 1978. 151(2): p. 353-68.

87. Zhang, J. and C.A. Piantadosi, *Mitochondrial oxidative stress after carbon monoxide hypoxia in the rat brain.* J. Clin. Invest., 1992. 90(4): p. 1193-9.

88. Mendelman, A., et al., *Protection of rat brain against exposure to CO afforded by barbiturate anesthesia. (Abstract).* Isr. J. Med. Sci., 1996. 32: p. 832.

89. MacMillan, V., *Regional cerebral blood flow of the rat in acute carbon monoxide intoxication.* Can J Physiol Pharmacol, 1975. 53(4): p. 644-50.

90. Mayevsky, A., *Cerebral blood flow and brain mitochondrial redox state responses to various perturbations in gerbils.* Adv. Exp. Med. Biol., 1992. 317: p. 707-716.

91. Koehler, R.C., et al., *Role of O_2-hemoglobin affinity on cerebrovascular response to carbon monoxide hypoxia.* Am J Physiol, 1983. 245(6): p. H1019-23.

92. Meilin, S., et al., *Effects of carbon monoxide exposure on the brain may be mediated by nitric oxide.* J. Appl. Physiol., 1996. 81: p. 1078-1083.

93. Toyoda, K., et al., *Effect of aging on regulation of brain stem circulation during hypotension.* J Cereb Blood Flow Metab, 1997. 17(6): p. 680-5.

94. Fujishima, M., et al., *Autoregulation of cerebral blood flow in young and aged spontaneously hypertensive rats (SHR).* Gerontology, 1984. 30(1): p. 30-6.

95. Mayevsky, A., *Biochemical and physiological activities of the brain as in vivo markers of brain pathology*, in *Cerebral Revascularization*, E.F. Bernstein, et al., Editors. 1993, Med-Orion Pub. p. 51-69.

96. Mayevsky, A., N. Zarchin, and J. Sonn, *Brain redox state and O_2 balance in experimental spreading depression and ischemia*, in *Migraine - Basic Mechanisms and Treatment* A. Lehmenkuhler, K.-H. Grotemeyer, and F. Tegtmeier, Editors. 1993, Urban & Schwarzenberg: Munchen-Wier, Baltimore. p. 379-393.

97. Wang, R. and L. Wu, *The chemical modification of KCa channels by carbon monoxide in vascular smooth muscle cells.* J Biol Chem, 1997. 272(13): p. 8222-6.

98. Wilkinson, J.H., J.W. Hopewell, and H.S. Reinhold, *A quantitative study of age-related changes in the vascular architecture of the rat cerebral cortex.* Neuropathol Appl Neurobiol, 1981. 7(6): p. 451-62.

99. Buerk, D.G. and P. Nair, *PtiO_2 and CMRO_2 changes in cortex and hippocampus of aging gerbil brain.* J. Appl. Physiol., 1993. 74(4): p. 1723-8.

100. Davis, M., et al., *Experimental stroke and neuroprotection in the aging rat brain.* Stroke, 1995. 26(6): p. 1072-8.

URL: http://dx.doi.org/10.14738/bjhmr.112.16760.

101. Ohata, M., et al., *Regional cerebral blood flow during development and ageing of the rat brain.* Brain, 1981. 104(2): p. 319-32.

102. Parmacek, M.S., et al., *Effect of aging on brain respiration and carbohydrate metabolism of CBF1 mice.* Gerontology, 1979. 25(4): p. 185-91.

103. Sylvia, A.L. and M. Rosenthal, *Effects of age on brain oxidative metabolism in vivo.* Brain Res., 1979. 165: p. 235-248.

104. Thom, S.R., S.T. Ohnishi, and H. Ischiropoulos, *Nitric oxide released by platelets inhibits neutrophil B2 integrin function following acute carbon monoxide poisoning.* Toxicol Appl Pharmacol, 1994. 128(1): p. 105-10.

105. Bures, J., O. Buresova, and J. Krivanek, *The Mechanism and Applications of Leão's Spreading Depression of Electroencephalographic Activity*. 1974, New York: Academic.

106. Mendelman, A., et al., *Blood flow and ionic responses in the awake brain due to carbon monoxide.* Neurol. Res., 2002. 24(8): p. 765-772.

107. Mayevsky, A., et al., *Interrelation between hyperbaric oxygenation and carbon monoxide intoxication in the rat brain in vivo*, in *Basic and Applied High Pressure Biology*, P.B. Bennett and R.E. Marquis, Editors. 1993, University of Rochester Press. p. 409-420.